

**UNIVERSIDADE ESTADUAL DO NORTE FLUMINENSE DARCY RIBEIRO
CENTRO DE BIOCÊNCIAS E BIOTECNOLOGIA – CBB
LABORATÓRIO DE CIÊNCIAS AMBIENTAIS – LCA
PÓS-GRADUAÇÃO EM ECOLOGIA E RECURSOS NATURAIS – PPGERN**

**DETERMINAÇÃO DE CARBONO NEGRO SEDIMENTAR A NÍVEL
MOLECULAR EM ZONAS COSTEIRAS TROPICAIS**

TASSIANA SOARES GONÇALVES SERAFIM

Orientador: Prof. Carlos Eduardo de Rezende (LCA/CBB/UENF)

CAMPOS DOS GOYTACAZES – RJ

Setembro – 2021

TASSIANA SOARES GONÇALVES SERAFIM

**DETERMINAÇÃO DE CARBONO NEGRO SEDIMENTAR A NÍVEL
MOLECULAR EM ZONAS COSTEIRAS TROPICAIS**

Dissertação apresentada ao Centro de Biociências e Biotecnologia da Universidade Estadual do Norte Fluminense Darcy Ribeiro como parte das exigências para a obtenção do título de Mestre em Ecologia e Recursos Naturais.

Orientador: Prof. Carlos Eduardo de Rezende

CAMPOS DOS GOYTACAZES – RJ

Setembro – 2021

FICHA CATALOGRÁFICA

UENF - Bibliotecas

Elaborada com os dados fornecidos pela autora.

S481 Serafim, Tassiana Soares Gonçalves.

DETERMINAÇÃO DE CARBONO NEGRO SEDIMENTAR A NÍVEL MOLECULAR EM ZONAS COSTEIRAS TROPICAIS / Tassiana Soares Gonçalves Serafim. - Campos dos Goytacazes, RJ, 2021.

56 f. : il.
Inclui bibliografia.

Dissertação (Mestrado em Ecologia e Recursos Naturais) - Universidade Estadual do Norte Fluminense Darcy Ribeiro, Centro de Biociências e Biotecnologia, 2021.
Orientador: Carlos Eduardo de Rezende.

1. Carbono negro. 2. Zonas costeiras. 3. Sedimento. 4. Ácidos benzeno-policarboxílicos. I. Universidade Estadual do Norte Fluminense Darcy Ribeiro. II. Título.

CDD - 577

DETERMINAÇÃO DE CARBONO NEGRO SEDIMENTAR A NÍVEL MOLECULAR EM ZONAS COSTEIRAS TROPICAIS

TASSIANA SOARES GONÇALVES SERAFIM

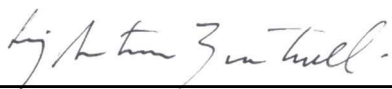
Dissertação apresentada ao Centro de Biociências e Biotecnologia da Universidade Estadual do Norte Fluminense Darcy Ribeiro como parte das exigências para a obtenção do título de Mestre em Ecologia e Recursos Naturais. Aprovada em 14 de setembro de 2021.

Comissão examinadora:



Dr. Carlos Eduardo de Rezende
Professor Titular
Universidade Estadual do Norte Fluminense
Darcy Ribeiro
Centro de Biociências e Biotecnologia
Laboratório de Ciências Ambientais
Matrícula Funcional: 641383-5

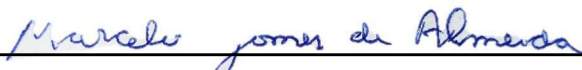
Dr. Carlos Eduardo de Rezende – Orientador – (LCA/CBB/UENF)



Dr. Luiz Antônio Martinelli – (CENA/USP)



Dr. Thorsten Dittmar – (ICBM/University of Oldenburg)



Dr. Marcelo Gomes de Almeida – (LCA/CBB/UENF)

AGRADECIMENTOS

Agradeço à Deus, pela minha vida, e por me permitir ultrapassar todos os obstáculos encontrados ao longo da realização deste trabalho. Pela saúde e por toda determinação para não desanimar em tempos de pandemia. À minha família, que sempre me incentivou e apoiou os meus sonhos, em especial ao meu pai.

Agradeço enormemente ao meu orientador, Carlos Eduardo de Rezende, pelo desempenho da função com máxima dedicação e amizade. Agradeço pelos ensinamentos e pela oportunidade! Sem a sua orientação este trabalho não poderia ter sido desenvolvido, ele nunca mediu esforços para ajudar e ensinar aos seus alunos e sou muito grata por fazer parte de seu grupo! Ao Jomar Marques e ao Marcelo Almeida, por toda paciência, ensino e carinho, que me ajudaram e me guiaram durante todo o meu aprendizado! Sinto enorme gratidão por tê-los em minha vida pessoal e profissional.

Agradeço também ao professor Gérard Thouzeau da Université de Brest pela coleta dos sedimentos superficiais na Guiana Francesa e por todo o ensinamento durante a campanha em 2019, meu sincero *merci beaucoup*. Ao professor Thorsten Dittmar e seu grupo do Institute for Chemistry and Biology of the Marine Environment, da Carl von Ossietzky University Oldenburg, por me receberem tão bem e me ajudarem na obtenção de parte dos dados que compõem a minha dissertação, *danke schön*.

Aos meus amigos, por toda a leveza que vocês trouxeram para minha vida nestes dois anos atípicos, também pelas risadas, consolos, ensinamentos e momentos compartilhados. Vocês são demais! Obrigada por me escutarem falar sobre carbono negro tantas e tantas vezes. Um especial “obrigada” ao Michael Seidel, por ter estado a meu lado mesmo tão distante, por todas as palavras de incentivo e por todo amor compartilhado.

À Universidade Estadual do Norte Fluminense Darcy Ribeiro, ao Programa de Pós-Graduação em Ecologia e Recursos Naturais e ao Laboratório de Ciências Ambientais, que foram essenciais no meu processo de formação com ensino público e de qualidade!

À Coordenação de Aperfeiçoamento de Pessoal de Nível Superior – Brasil (CAPES) – Código de Financiamento 001 – pela bolsa concedida.

SUMÁRIO

LISTA DE FIGURAS	vi
LISTA DE TABELAS	viii
RESUMO	ix
ABSTRACT	x
1. INTRODUÇÃO GERAL	1
2. OBJETIVO	5
3. RESULTADOS	6
3.1. Artigo científico: Carbon isotopic composition and black carbon dynamics in surface sediments under Amazon and Atlantic rainforest influence	6
Carbon isotopic composition and black carbon dynamics in surface sediments under Amazon and Atlantic rainforest influence	7
INTRODUCTION	9
MATERIALS AND METHODS	11
Study Area	11
The Amazon and French Guiana Coastal Zones	11
The Paraíba do Sul Coastal Zone	12
Sampling	13
Elemental and isotopic composition of organic matter	14
Black Carbon Determination	14
Sources of organic matter in coastal sediments	15
Burial Flux	16
Statistical Analyses	17
RESULTS	17
Sources of organic matter in coastal sediments	17
BC in coastal zones	19
DISCUSSION	20
Sources of organic matter in coastal sediments	20
BC in coastal zones	23
Sources for BC and burial flux	25
REFERENCES	28
SUPPLEMENTARY INFORMATION	40
4. CONSIDERAÇÕES FINAIS	43
5. REFERÊNCIAS BIBLIOGRÁFICAS	43

LISTA DE FIGURAS

INTRODUÇÃO GERAL

- Figura 1.** Modelo do "contínuo" de combustão de CN. Adaptado de Hedges et al. (2000) e Masiello (2004). 1
- Figura 2.** Ácidos benzeno policarboxílicos formados a partir da oxidação da molécula de CN. Modificado de Brodowski et al. (2005). 4
- Figura 3.** Conteúdo de CN (círculos brancos, escala direita) produzidos a temperaturas crescentes de carbonização e a contribuição relativa do BPCA individual para o conteúdo total do carbono negro (escala esquerda). Modificado de Schneider et al. (2010). 5

Artigo científico

- Figure 1.** Map representation of the coastal areas of the Sinnamary estuary in French Guiana (B), the Amazonas plume in northern Brazil (D), and the PSR in southeastern Brazil (C). 13
- Figure 2.** Boxplot representation of $\delta^{13}\text{C}$ values (A) and their distribution along the electrical conductivity gradient for the Sinnamary, Amazon, and PSR coastal zones (B). Different letters upon the boxplots represent statistical support for difference of the mean (Tukey's test, $p < 0.05$) and circles represent outliers (A). Linear regressions of the models were $Y = -26.48 + 0.00002 X$, $Y = -27.14 + 0.00007 X$, and $Y = -22.89 + 0.00002 X$ for the Sinnamary, Amazon, and PSR coastal zones, respectively (B). The highlighted symbols were not used in the construction of the models. 18
- Figure 3.** Boxplot representation of BC values normalized by OC content (A) and degree of condensation (B). BC content (C) and degree of condensation (D) along the electrical conductivity gradient in the coastal areas of the Sinnamary, the Amazon, and the PSR. Different letters upon the boxplots represent statistical support for difference of the mean (Tukey's test, $p < 0.05$) and circles represent outliers (A and B). The linear regressions of the models for BC were $Y = 1.17 - 0.00006 X$, $Y = 0.31 + 0.0000002 X$, and $Y = 0.47 + 0.00001 X$ for the Sinnamary, Amazon and PSR coastal zones, respectively (C). Models of the degree of condensation were constructed from the equations: $Y = 0.81 - 0.00004 X$, $Y = 0.05 + 0.0000056 X$, and $Y = 0.55 - 0.000001 X$ for the Sinnamary, Amazon, and PSR

coastal zones, respectively (D). The highlighted symbols were not used in the construction of the model.....20

Figure 4. $\delta^{13}\text{C}$ vs. $(\text{C:N})_a$ (A) and $\delta^{13}\text{C}$ vs. $\delta^{15}\text{N}$ (B) in the coastal zones of the Sinnamary, Amazon, and PSR. End Members sources from Ometto et al. (2006), Hamilton and Lewis (1992), Bouillon et al. (2011), Ribas (2012), Ellis et al. (2012) and Caraballo et al. (2014) and Ray et al. (2018).....22

Figure 5. Contribution of terrestrial C_3 plant for the OM vs. BC content to the coastal zones of the Sinnamary, Amazon, and PSR. The linear regressions of the models were $Y = -1.818 + 0.004 X$, $Y = -0.056 + 0.008 X$, and $Y = 1.274 - 0.016 X$ for the Sinnamary, Amazon, and PSR coastal zones, respectively. The highlighted symbols were not used in the construction of the models.....26

LISTA DE TABELAS

Artigo Científico

Supplementary Table 1. Sampling locations (latitude and longitude), electrical conductivity ($\mu\text{S cm}^{-1}$), carbon and nitrogen isotopic compositions ($\delta^{13}\text{C}$ and $\delta^{15}\text{N}$, respectively), carbon and nitrogen atomic ratio, black carbon content normalized by organic carbon content and degree of condensation (B6CA:B5CA).....	40
Supplementary Table 2. Isotopic fractionation factors for carbon and nitrogen isotopic compositions used on the MixSIAR model for each coastal zone.....	42

RESUMO

A modificação do uso do solo de floresta para plantações e áreas de pastagem além de modificar a paisagem, altera a qualidade da matéria orgânica (MO) do solo. Atualmente, cerca de 15 e 74 % dos biomas da Amazônia e Mata Atlântica, respectivamente, apresentam uma forte modificação da paisagem como consequência às alterações antrópicas. Uma estratégia muito utilizada para remoção de biomassa florestal e manejo das áreas de plantações e de pastagem é a utilização do fogo. A combustão incompleta da biomassa produz MO termicamente modificada que, globalmente, representa cerca de 14 % da MO encontrada no solo, e é comumente denominada de carbono negro (CN). A entrada de CN associado às partículas nos sistemas aquáticos ocorre a partir do transporte lateral e, sua deposição no compartimento sedimentar ocorre ao longo do gradiente continente-oceano. O trabalho investigou a dinâmica e a concentração de CN em sedimentos de zonas costeiras em bacias de drenagem principalmente cobertas por florestas (plantas C₃): zonas costeiras dos rios Sinnamary (FG_{CZ}) e Amazonas (AM_{CZ}), e na zona costeira do rio Paraíba do Sul (PSR_{CZ}), coberta principalmente por gramíneas (plantas C₄) devido às modificações antrópicas. Para identificar as fontes que contribuem para a MO sedimentar, a composição isotópica de carbono ($\delta^{13}\text{C}$) foi determinada a partir do analisador elementar Flash 2000 acoplado a um espectrômetro de massa Delta V e o CN foi determinado a partir da oxidação da MO e formação de seus marcadores moleculares nos equipamentos: GC-MS e HPLC. O $\delta^{13}\text{C}$ da PSR_{CZ} apresentou valores enriquecidos em ^{13}C ($-22,6 \pm 1,3 \text{ ‰}$, $p < 0,01$) quando comparados as AM_{CZ} e FG_{CZ} ($-25,0 \pm 3,1$ e $-26,1 \pm 1,0 \text{ ‰}$, respectivamente), indicando que a alteração do uso do solo na bacia pode estar modificando a MO transportada. O teor de CN, normalizado ao teor de carbono orgânico (CO) do sedimento, foi menor na AM_{CZ} ($0,32 \pm 0,24 \text{ mg g}^{-1} \text{ CO}$), provavelmente devido à alta descarga do rio e a deposição de CN em locais intermediários. FG_{CZ} e PSR_{CZ} apresentaram concentrações semelhantes de CN ($0,73 \pm 0,67$ e $0,95 \pm 0,74 \text{ mg g}^{-1} \text{ OC}$, respectivamente, $p = 0,759$), mas com fontes diferindo de acordo com a atual cobertura vegetal das bacias. Na FG_{CZ}, o CN foi rapidamente degradado ao longo do gradiente de condutividade elétrica (EC), o que sugere que o CN pode ser composto principalmente de carbono lábil susceptível à degradação rápida. Na PSR_{CZ}, o conteúdo de CN aumenta no gradiente EC e o grau de condensação não varia, indicando dominância de carbono estável e possível deposição atmosférica de fuligem. Na AM_{CZ}, o conteúdo de CN não varia ao longo do gradiente EC, mas o grau de condensação mostra que a deposição de CN pode ter dois mecanismos: CN envelhecido do transporte fluvial e remoção do componente hidrofóbico do CN dissolvido. Amostras com altos valores de EC exibiram teor de CN, o que evidencia o transporte de material terrestre refratário para as zonas costeiras.

ABSTRACT

The land-use change from forest to cultivated plantations and pasture areas, besides modifying the landscape, alters the quality of organic matter (OM) in the soil. Currently, about 15 and 74 % of the Amazon and Atlantic Forest biomes, respectively, present a strong modification of the landscape as a consequence of anthropogenic alterations. A widely used strategy for removing forest biomass and managing plantation and pasture areas is the use of fire. The incomplete combustion of biomass produces thermally modified OM which, globally, represents about 14 % of the OM present in the soil, and is commonly known as black carbon (BC). The input of particle-associated BC into aquatic systems occurs from lateral transport and, its deposition into the sediment compartment occurs along the continent-ocean gradient. The study investigated the dynamics and concentration of BC in sediments of coastal zones in drainage basins mainly covered by forests (C_3 plants): coastal zones of the Sinnamary (FG_{CZ}) and Amazon rivers (AM_{CZ}), and in the coastal zone of the Paraíba do Sul river (PSR_{CZ}), covered mainly by grasses (C_4 plants) due to anthropogenic modifications. To identify the sources contributing to the sediment OM, the carbon isotopic composition ($\delta^{13}C$) was determined from the Flash 2000 elemental analyzer coupled to a Delta V mass spectrometer, and BC was determined from the oxidation of OM and formation of its molecular markers in the equipment: GC-MS and HPLC. The $\delta^{13}C$ of the PSR_{CZ} showed ^{13}C -enriched values (-22.6 ± 1.3 ‰, $p < 0.01$) when compared to the AM_{CZ} and FG_{CZ} (-25.0 ± 3.1 and -26.1 ± 1.0 ‰, respectively), indicating that land-use change in the basin may be modifying the transported OM. The BC content, normalized to the organic carbon (OC) content of the sediment, was lower in the AM_{CZ} (0.32 ± 0.24 mg g⁻¹ OC), probably due to the high river discharge and the deposition of BC at intermediate sites. FG_{CZ} and PSR_{CZ} showed similar BC content (0.73 ± 0.67 and 0.95 ± 0.74 mg g⁻¹ OC, respectively, $p = 0.759$), but with sources differing according to the current vegetation cover of the basins. In the FG_{CZ} , BC has rapidly degraded along with the electrical conductivity (EC) gradient, suggesting that BC may be composed mainly of labile carbon susceptible to rapid degradation. In the PSR_{CZ} , BC content increases along the EC gradient, and the degree of condensation does not vary, indicating the dominance of stable carbon and possible atmospheric soot deposition. In the AM_{CZ} , BC content does not vary along the EC gradient, but the degree of condensation shows that BC deposition may have two mechanisms: aged BC from river transport and removal of the hydrophobic component of dissolved BC. Samples with high EC values exhibited BC content, which evidences the transport of refractory terrestrial material to the coastal zones.

1. INTRODUÇÃO GERAL

Incêndios florestais e queima de vegetação atingem anualmente cerca de 4 % da biomassa global (Randerson et al., 2012). A queima incompleta de biomassa vegetal produz uma forma enriquecida em carbono que apresenta caráter refratário e pode ser resistente à degradação: o carbono negro (CN; Goldberg, 1985). Estas características somadas à sua presença em todos os compartimentos ambientais o torna um importante componente do ciclo do carbono (Bird e Ascough, 2012; Santín et al., 2016; Coppola et al., 2018). O CN é comumente apresentado como um modelo de combustão contínua onde os produtos variam desde matéria orgânica levemente alterada a compostos aromáticos policíclicos altamente condensados (Figura 1; Masiello, 2004; Coppola e Druffel, 2016). Todos os compostos deste modelo apresentam elevado conteúdo de carbono e são quimicamente heterogêneos (Masiello, 2004). Esta heterogeneidade e a alta complexidade resultam na elevada resistência à oxidação química e térmica e em diferentes taxas de reatividade da molécula (Schmidt e Noack, 2000; Jones et al., 2017) diferindo da matéria orgânica não termicamente alterada (Glaser et al., 1998). A característica inerte é observada principalmente nos compostos mais condensados do modelo, o que resulta na baixa formação de CO₂ fazendo com que o CN se torne um sumidouro de carbono (Forbes et al., 2006).

Características	Matéria orgânica levemente carbonizada	Matéria orgânica carbonizada	Carvão vegetal	Cinza	Grafite
Tamanho	mm ou maior		mm a µm	µm	
Reservatório inicial	solos		solos e atmosfera		
Alcance	m	m a km		km	
Reatividade: (O:C) _a	0,8	0,6	0,4	0,2	0

Figura 1. Modelo do "contínuo" de combustão de CN. Adaptado de Hedges et al. (2000) e Masiello (2004).

O CN produzido em bacias de drenagem compõem, a nível mundial, cerca de 14 % da matéria orgânica do solo (Reisser et al., 2016) e, de acordo com Kuhlbusch e Crutzen (1995), aproximadamente 80 % do material pirogênico produzido fica inicialmente no solo próximo ao local de produção. O tempo de residência no solo pode chegar a centenas de anos e a variação das taxas de decomposição de CN encontradas é resultado dos diferentes mecanismos que podem modificar fisicamente e quimicamente a molécula de CN (Singh et al., 2012; Wang et al., 2013), bem como sua estabilização em escala local (Wang et al., 2016). A remoção de CN do solo e a entrada no sistema aquático, se dão através de sua solubilização por ação de organismos microbianos (Dittmar et al., 2012) e pelo transporte lateral de partículas (Major et al., 2010) que ocorre principalmente após erosão e consequente lixiviação do solo após eventos de precipitação. Além disso, os compostos altamente condensados podem também ser transportados via atmosfera na forma de fuligem e serem depositados longe de seu local de produção (Figura 1; Masiello, 2004). Assim, a presença de CN em rios, zonas de transição e no oceano se devem também à deposição atmosférica e não somente ao transporte fluvial (Hockaday et al., 2007; Coppola et al., 2014), embora este seja o processo majoritário na mobilização de CN para esses ecossistemas aquáticos (Forbes et al., 2006; Coppola et al., 2018).

Sistemas fluviais através de suas zonas estuarinas conectam os ciclos de carbono terrestre e marinho (Coppola et al., 2018) transportando cerca de 2,7 Pg de carbono terrestre por ano para os oceanos (Aufdenkampe et al., 2011). Parte deste carbono orgânico é conservado ao longo do gradiente continente – oceano e, o CN compõe cerca de 10 e 16 % do carbono orgânico dissolvido e particulado encontrados em rios, respectivamente (Jaffé et al., 2013; Coppola et al., 2018; Jones et al., 2019). A fração particulada está constantemente sujeita a deposição acarretando no acúmulo de CN no compartimento sedimentar ao longo do gradiente (Schmidt e Noah, 2000). No sedimento, o CN pode constituir até 50 % do carbono orgânico (Middelburg et al., 1999) adsorvido principalmente nas partículas finas, como silte e argila. Entretanto, no compartimento sedimentar marinho sua mobilização representa de 3 a 10 % do fluxo global de CN (Santín et al., 2016). Em consequência ao forte gradiente físico-químico das zonas estuarinas, tem-se a redução considerável do transporte de partículas para o oceano. Em um estudo realizado por Regnier et al. (2013), foi estimado o fluxo de transporte lateral de

partículas ao longo do gradiente continente – oceano e, os autores relataram que globalmente, 50 % do carbono orgânico particulado não alcança o oceano devido à sua deposição em zonas de transição facilitada pelo forte gradiente físico – químico.

Com a finalidade de determinar o CN, diversos métodos analíticos são encontrados na literatura, abordando diferentes espectros do modelo de combustão contínua (Masiello, 2004; Hammes et al., 2007). O método de determinação de CN a partir dos ácidos benzeno-policarboxílicos (BPCA) atua em quase todo o modelo e determina especificamente as porções aromáticas condensadas (Dittmar et al., 2012). Sánchez-García et al. (2013) avaliaram a concentração de CN em sedimentos do golfo de Cádiz (Espanha) comparando dois métodos na determinação de CN: a partir dos BPCA e a partir de termo oxidação (GBC), este identifica a porção mais aromática do “contínuo”. Os autores encontraram diferentes concentrações de CN devido à diferença da amplitude da determinação dos compostos. No método utilizando os marcadores moleculares, o CN compôs 11 ± 10 % do carbono orgânico, enquanto o método GBC o material pirogênico compunha 5 ± 3 %, assim, a comparação entre diferentes métodos pode levar a subestimação do conteúdo de CN.

Os marcadores moleculares de CN são obtidos a partir da oxidação da molécula com ácido nítrico em alta temperatura e pressão com posterior isolamento e quantificação dos BPCA para estimar o conteúdo de CN e, são considerados marcadores específicos para determinação à nível molecular de CN (Dittmar, 2008). A oxidação converte o CN em anéis de benzeno que apresentam números de grupos de ácidos carboxílicos que podem variar entre 3 a 6 grupos (Figura 2; Brodowski et al., 2005).

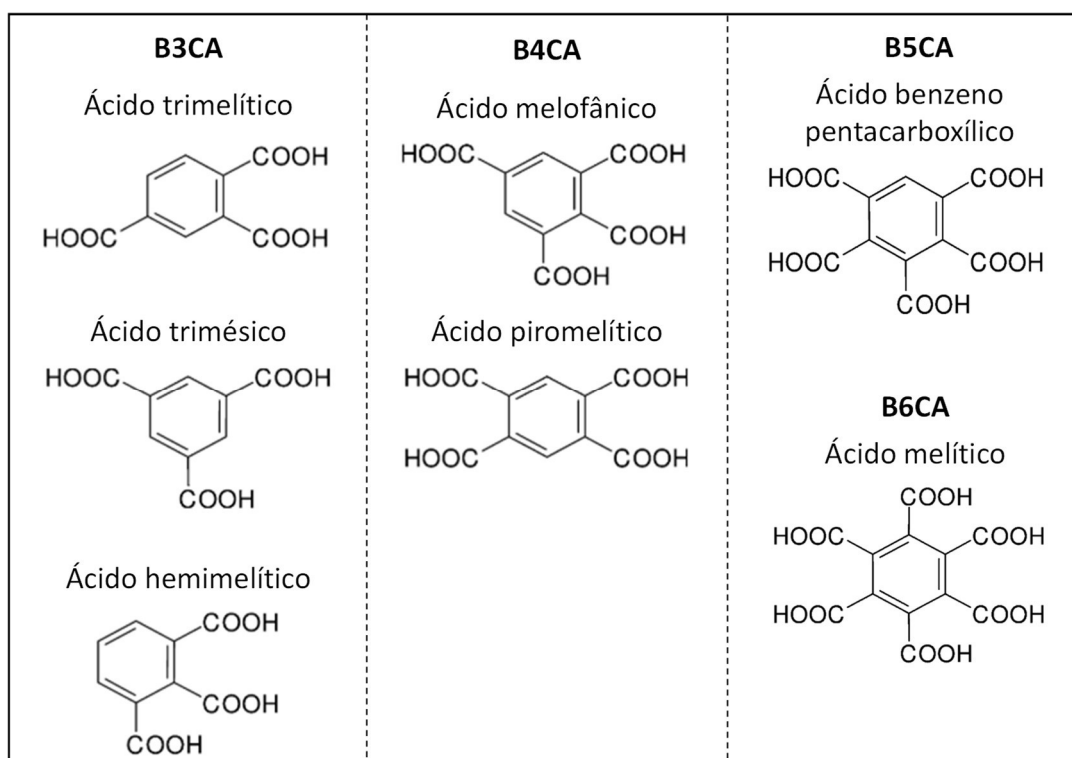


Figura 2. Ácidos benzeno policarboxílicos formados a partir da oxidação da molécula de CN. Modificado de Brodowski et al. (2005).

Ao avaliar a existência de um padrão sistemático na produção de BPCA, Schneider et al. (2010) avaliaram sua distribuição em intervalos de temperatura de combustão de biomassa variando entre 200 e 1000 °C. Os autores observaram um aumento da produção dos grupos com 5 e 6 ácidos carboxílicos, ácidos benzeno pentacarboxílico (B5CA) e melítico (B6CA), respectivamente, com o aumento da temperatura, além do aumento do conteúdo de CN (Figura 3). Embora a temperatura de combustão pareça reger as propriedades físicas e químicas da matéria orgânica termicamente modificada (Brown et al., 2006), outros parâmetros podem também influenciar na produção, tais como: tipo de fonte de biomassa vegetal, oxigênio, duração da combustão e/ou condições do vento (Schneider et al., 2010; Wolf et al., 2013; Budai et al., 2017). A faixa de temperaturas típicas para queima de biomassa próximo à superfície do solo varia de 275 a 500 °C e pode alcançar 800 °C para incêndios de vegetação arbórea (Alexis et al., 2007), nestas circunstâncias, o B5CA e o B6CA compõem entre 70 e 95 % da molécula de CN gerado a partir da queima incompleta de biomassa vegetal (Schneider et al., 2010).

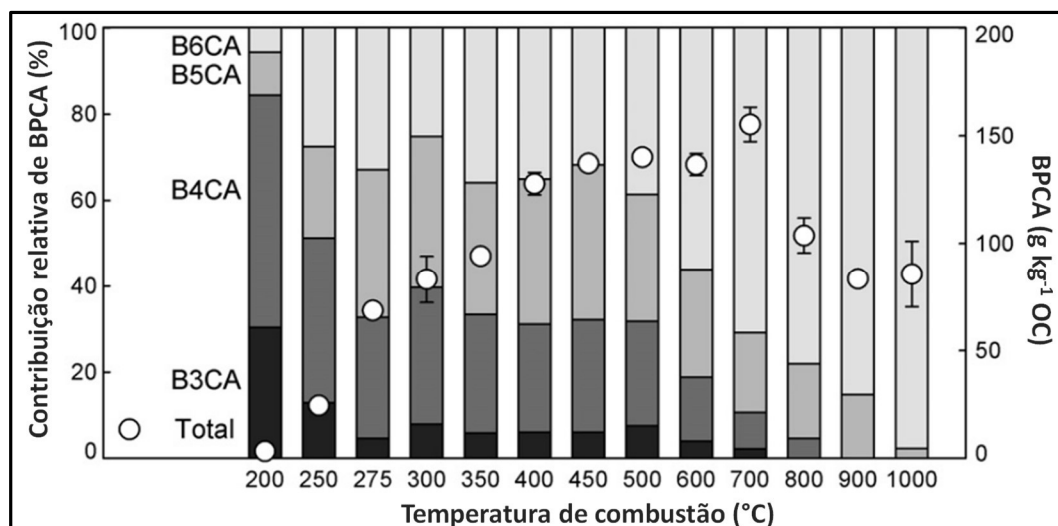


Figura 3. Conteúdo de CN (círculos brancos, escala direita) produzidos a temperaturas crescentes de carbonização e a contribuição relativa do BPCA individual para o conteúdo total do carbono negro (escala esquerda). Modificado de Schneider et al. (2010).

A contribuição individual dos marcadores moleculares de CN é usada para avaliar o tamanho dos compostos aromáticos de uma amostra ou o seu grau de condensação. Enquanto que os marcadores B3CA, B4CA e B5CA podem ser produzidos a partir de anéis na margem externa da molécula, o B6CA só é originado a partir de seu núcleo (Schneider et al., 2010). Apesar deste método avaliar quantitativamente e qualitativamente os marcadores moleculares, o método apresenta algumas limitações: em amostras com peso de CO superior a 5 mg, os BPCA são produzidos a partir de MO não termicamente modificada (Kappenberg et al., 2016). Portanto, ao avaliar a concentração e a dinâmica do CN e comparar com outros trabalhos essas limitações (bem como uso de diferentes técnicas) devem ser consideradas a fim de não superestimar ou subestimar os processos que ocorrem desde a produção ao destino final do CN.

2. OBJETIVO

O trabalho teve como objetivo geral analisar o conteúdo de CN e sua dinâmica em zonas costeiras de rios com coberturas vegetais distintas a partir da determinação do CN a nível molecular.

2.1. Objetivos específicos

Avaliar através da ferramenta dos isótopos estáveis do carbono e nitrogênio as fontes que contribuem para a matéria orgânica do compartimento sedimentar das zonas costeiras estudadas e, adicionalmente, avaliar se a ferramenta isotópica pode ajudar a elucidar a questão acerca da produção de CN nas bacias de drenagem.

3. RESULTADOS

Os resultados produzidos durante o período de mestrado serão apresentados na forma de artigo científico a seguir:

- 3.1. Artigo científico: **Carbon isotopic composition and black carbon dynamics in surface sediments under Amazon and Atlantic rainforest influence**

Carbon isotopic composition and black carbon dynamics in surface sediments under Amazon and Atlantic rainforest influence

Serafim, T.S. G.^{a*}, Almeida, M., G.^a, Thouzeau, G.^b, Michaud, E.^b, Seidel, M.^c, Dittmar, T.^c, Rezende, C. E.^a

^aLaboratório de Ciências Ambientais, Centro de Biociências e Biotecnologia, Universidade Estadual do Norte Fluminense Darcy Ribeiro, Campos dos Goytacazes RJ, CEP 28013-602, Brazil.

^bUniv Brest, CNRS, IRD, Ifremer, LEMAR, F-29280 Plouzané, France.

^cResearch Group for Marine Geochemistry (ICBM—MPI Bridging Group), Institute for Chemistry and Biology of the Marine Environment, Carl von Ossietzky University Oldenburg, Germany.

*Corresponding author: Serafim, T.S.G., e-mail: tassiana.sgs@gmail.com

Abstract: Our research investigated the dynamics and concentration of black carbon (BC) and the carbon isotopic composition ($\delta^{13}\text{C}$) of organic matter (OM) in coastal sediments in drainage basins mainly covered by forested (Amazon Rainforest – C_3 plants): coastal zones of the Sinnamary and Amazon River; as well as the coastal zone of the Paraíba do Sul River (PSR), which is mainly covered by grasses (Atlantic Rainforest – C_4 plants). The results showed the $\delta^{13}\text{C}$ was more ^{13}C -enriched in PSR coastal sediments ($-22.6 \pm 1.3 \text{‰}$, $p < 0.01$) when compared to the Amazon and Sinnamary ($-25.0 \pm 3.1 \text{‰}$ and $-26.1 \pm 1.0 \text{‰}$, respectively), indicating that the land-use changes in the basin have probably modified the quality of OM in the sediment of PSR coastal zone. BC content, normalized by the organic carbon content, was lower in the Amazon sediments ($0.32 \pm 0.24 \text{ mg g}^{-1} \text{ OC}$). The Sinnamary and PSR coastal zones had similar concentrations (0.73 ± 0.67 and $0.95 \pm 0.74 \text{ mg g}^{-1} \text{ OC}$, respectively), but the sources for BC content differed according to the vegetation cover of the basins. Along with the electrical conductivity (EC) gradient, BC content decreased in the Sinnamary coastal zone, suggesting that BC might be susceptible to faster degradation. In the PSR coastal zone, the BC content increased, while the degree of condensation did not change, indicating stable carbon dominance and possible atmospheric deposition of soot. In the Amazon coastal zone, BC content did not change along the EC gradient, but the degree of condensation showed that BC in sediments may have two mechanisms: aged BC from river transport and removal of the hydrophobic component of dissolved BC. Different sources and transformations act on the concentrations and dynamics of BC in coastal zones.

Keywords: Black carbon, Amazon Rainforest, Atlantic Rainforest, Carbon isotopic composition, Sediments.

INTRODUCTION

In Brazil, the conversion of primary forest areas for cropland and agriculture has devastated the Atlantic rainforest and continues to destroy important biomes such as the world's largest forest, the Amazon rainforest (Ferrante and Fearnside, 2019), modifying qualitatively the organic matter (OM) present in the soil (Bernardes et al., 2004). The conversion of native forest vegetation has altered the Atlantic rainforest landscape, of which about 28 % of its original vegetation cover remains distributed in fragments (Rezende et al., 2018; Solórzano et al., 2021). Such anthropogenic areas currently comprise approximately 15 % of the Amazon biome (Stahl et al., 2016) and are increasing due to the invasion of forest areas. One strategy for forest biomass removal and the management of anthropic areas is the use of fire as a tool (Edwards, 1984), which is the main vector for biomass removal in the Amazon rainforest today through forest fires caused by drought events (Aragão et al., 2018) and anthropogenic activities, such as the management of cattle pasture and agricultural areas. It is estimated that globally anthropogenic forest fires and anthropogenic burning emit about 2.2 Pg of carbon per year into the atmosphere in the form of greenhouse gases (Werf et al., 2017). In addition, fires produce another carbon-enriched form that exhibits greater resistance to degradation compared to non-altered thermally OM, black carbon (Forbes et al., 2006; Bird and Ascough, 2012).

Black carbon (BC) is the commonly used term to describe the thermally altered OM produced after incomplete combustion of plant biomass or fossil fuels (Goldberg, 1985). Hedges et al. (2000) described the broad spectrum of BC compounds as a combustion "continuum" model, which was later described as a degradation continuum that varies from slightly altered biomass susceptible to rapid degradation to highly condensed aromatic compounds that can persist in the environment (Masiello, 2004; Bird et al., 2015). The global production of BC derived from plant biomass releases between 50 and 300 Tg of BC per year (Forbes et al., 2006; Bird et al., 2015) and it is estimated that 80 % of BC initially remains at its production site after combustion (Kuhlbusch and Crutzen, 1995). According to Reisser et al. (2016), globally, BC constitutes about 14 % of soil OM with an average residence time in the compartment of 88 years, in a period that can range from a few years to millennia, depending on the combination of physical, chemical, and

microbial processes taking place in the OM degradation (Singh et al., 2012). The removal of BC from the soil and its entry into the aquatic system occurs mainly through the transport of the dissolved phase after solubilization of historical BC (Dittmar, 2008; Dittmar et al., 2012) and lateral particle transport resulting mainly from soil erosion (Major et al., 2010). In addition, to a smaller extent, the input of BC into aquatic systems can occur via atmospheric transport, and its deposition can occur along the entire continent – ocean gradient (Jurado et al., 2008; Coppola et al., 2018).

Increased erosion due to land use conversion increases the transport of particles to the aquatic system, resulting in the global accumulation of 75 Tg per year of sediments from areas below 2000 m altitude (Wilkinson and McElroy, 2007; Bird et al., 2015). These eroded particles are deposited along the continent – ocean gradient, mostly in continental areas and in transition zones. About 20 % of this material reaches its final destination: the marine sediment compartment (Rumpel et al., 2009; Bird et al., 2015). By estimating the flux of BC in the particulate fraction of the water column and sediments of large (e.g., the Amazon, Congo) and small rivers (e.g., the Eel, Santa Clara, Danube), Coppola et al. (2018) observed that BC comprises about 15.8 ± 0.9 % of the organic carbon (OC) present in the suspended particulate matter (SPM) and sediments. Furthermore, the authors attributed the export dynamics of BC in the rivers as resulting from soil erosion.

The global flux of OC associated with SPM to the ocean ranges from 19 to 80 Tg per year (Bird et al., 2015). This flux and the quality of the pyrogenic material associated with the SPM to coastal zones can be influenced by the characteristics of rivers and their drainage basins (Burdige, 2007). In small rivers usually associated with mountains, narrow continental shelves, or active continental margins, the transport of eroded material to the coastal zone occurs more rapidly with relatively low remineralization rates of OM along the continent – ocean gradient (Blair et al., 2003; Burdige, 2007). In contrast, in large rivers and deltas, SPM is subject to cycles of deposition and resuspension, and as a result of these processes, there is increased remineralization of OM due to long residence times (Aller, 1998). Additionally, the OM (or BC) associated with the SPM transported can be replaced downstream by OM produced at lower elevations, and/or dilution can also affect its flux (Aller et al., 1996; Burdige, 2007). The transport of particles to the ocean is considerably reduced due to the strong physicochemical gradient in the estuarine

zones, which favors processes such as flocculation. Regnier et al. (2013), by analyzing the lateral transport flux of particulate matter to coastal zones, observed that, globally, 50 % of particulate OC does not reach the ocean due to its deposition in transition zones.

Thus, the present study sought to evaluate the dynamics and concentration of BC in the sediment compartment of coastal zones of basins with primary forest vegetation cover (terrestrial plants with photosynthetic cycle C_3): coastal zones of the Sinnamary and Amazon rivers; and, as a result of land-use change, a basin mostly covered by grasses (terrestrial plants photosynthetic cycle C_4): coastal zone of the Paraíba do Sul river (PSR), to evaluate if the modification of primary forest areas to pasture and cultivation areas changed the OM deposited in the sediment compartment of the coastal zone. To answer this question, we analyzed the content of BC using its molecular markers, the benzene-polycarboxylic acids (BPCA), as well as the determination of the elemental and isotopic compositions of bulk organic carbon (OC and $\delta^{13}C$, respectively) and nitrogen (N and $\delta^{15}N$, respectively) of the OM. We hypothesized that I: the PSR sample set presents $\delta^{13}C$ values ^{13}C -enriched due to the modification of the vegetation cover of the basin; II: that the BC content in the coastal zone of the Amazon River is lower as a result of the processes of dilution and replacement of OM from the floodplain; and III: the modification of land use in PSR coastal zone is directly related to the BC content.

MATERIALS AND METHODS

Study Area

The Amazon and French Guiana Coastal Zones

The Amazon rainforest extends over several countries, including French Guiana, and has an area representing about 45 % of the world's remaining tropical forests (Laurance et al., 2001), or approximately 4 % of the Earth's surface (about 6,100,000 km²) (Malhi et al., 2008; Gallo and Vinzon, 2015). In addition to playing an important role in carbon storage in the Amazon's vegetation biomass, the transport of terrestrial carbon to the ocean takes place via the Amazon River (Cai et al., 1988; Malhi et al., 2006; Malhi et al., 2008).

The Amazon River has a seasonal cycle with a maximum discharge reaching an average of $209,000 \text{ m}^3 \text{ s}^{-1}$ during the period from May to July (Latrubesse, 2008). The discharge of materials to the coastal zone comprises approximately 20 % of the global input of terrestrial material to the ocean (Richey et al., 1986; Ward et al., 2015). As a consequence of the basin climate, strong erosion and rapid particle deposition processes can lead to rapid changes in sedimentation rates in the Amazon River plume area (Kuehl et al., 1986). The plume moves in a northwestern direction, and some authors have suggested that a large part of the OM in the sedimentary compartment of the Brazilian shelf and adjacent northwestern areas originates from the Amazon basin (Wells and Coleman, 1981; Nittrouer et al., 1986). Approximately 20 % of the SPM reaching the coastal zone is carried towards French Guiana as a result of the interaction between the Brazilian North Current, the east trade winds, and semi-diurnal sea currents (Geyer et al., 1996; Aller et al., 2004).

Vegetation cover in French Guiana is 97 % tropical forest (Chave et al., 2001) with extensive mangrove forests that occur more than 80 % of the littoral (Fromard et al., 2004). The Sinnamary River, considered a small river, has an average discharge of $237 \text{ m}^3 \text{ s}^{-1}$ with its drainage basin extending over $6,565 \text{ km}^2$ (Richard et al., 2000; Luglia et al., 2019). The Sinnamary River estuary is under a macro tidal regime, with a tidal range around 3 m near its mouth (Ray et al., 2018), which increases the input of leached material from the estuary's extensive mangrove forest dominated by *Avicennia germinans* (Marchand et al., 2003, Marchand, 2017).

The Paraíba do Sul Coastal Zone

The Paraíba do Sul River (PSR) basin, with an area of $57,000 \text{ km}^2$, extends over the states of São Paulo, Rio de Janeiro, and Minas Gerais in the southeast region of Brazil (Ovalle et al., 2013). The PSR occupies an area that was previously and completely covered by the Atlantic rainforest and currently approximately 74 % of the basin is covered by pasture and sugarcane areas (Figueiredo et al., 2011; Marques et al., 2017). As a result of this change, the basin has suffered from an intense erosion process leading to an increase in the contribution of particles to the aquatic system. The PSR estuary and the second largest mangrove forest in the state of Rio de Janeiro are located in São João da Barra, in the Norte Fluminense

region (Bernini and Rezende, 2004). During the dry period, between June and September, the PSR exhibits discharge rates varying between 200 and 500 m³ s⁻¹, while reaching a maximum of 2,600 m³ s⁻¹ during the rainy period (Silva et al., 2001). The PSR is characterized as a small to medium-sized river.

Sampling

Surface sediment samples (0 - 2 cm) were collected following a gradient of electrical conductivity totaling 33 samples distributed in 6, 14, and 13 samples for the coastal zones of the Sinnamary estuary (5°21' - 5°30'N and 52°56' - 53°3'W), the Amazon plume (2°S - 4°N and 46° - 51°W), and the PSR coastal zone (21°28' - 21°40'S and 40°48' - 41°6'W), respectively (Figure 1; Supplementary Table 1). The sample sets were collected during the wet season: on January (2019), April (2018), and February (2014) for Sinnamary estuary, Amazon plume, and PSR coastal zone, respectively.

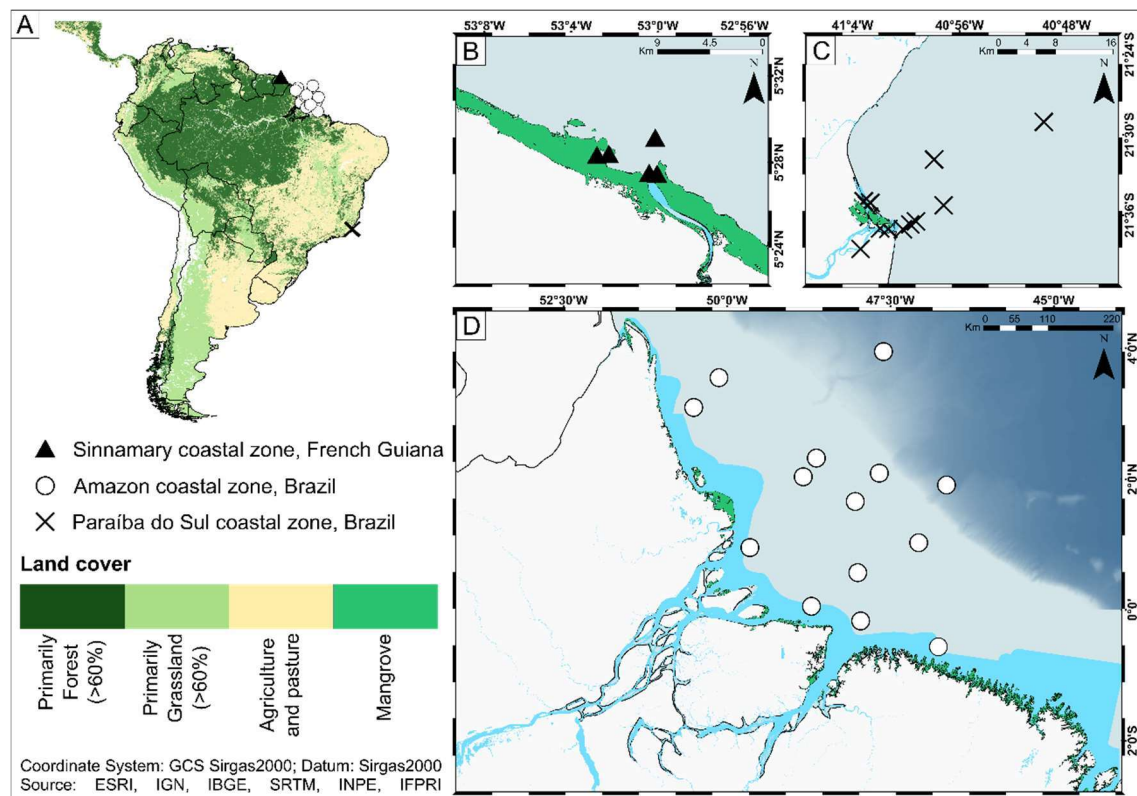


Figure 1. Map representation of the coastal areas of the Sinnamary estuary in French Guiana (B), the Amazonas plume in northern Brazil (D), and the PSR estuary in southeastern Brazil (C).

Elemental and isotopic composition of organic matter

The samples were freeze-dried at the laboratory and homogenized, and 10 mg of sediments were weighed into tin and silver capsules. To obtain OC content and $\delta^{13}\text{C}$ composition, the samples were acidified for decarbonation using 2M HCl in silver capsules. The samples were weighed into tin capsules to obtain N and $\delta^{15}\text{N}$ values. Elemental and isotopic values were obtained with the Flash 2000 elemental analyzer coupled to a Delta V mass spectrometer, with the detection limit for OC content and $\delta^{13}\text{C}$ of 0.05 % and N content and $\delta^{15}\text{N}$ values of 0.03 %.

Black Carbon Determination

The method used to determine black carbon was modified from Glaser et al. (1998) and Brodowski et al. (2005). The samples were pre-digested with 10 mL trifluoroacetic acid for 4 h in a high-pressure system at 100 ± 5 °C. The samples were filtered and the filters placed in an oven for 2 h under 40 °C temperature. After drying, for oxidation of the thermally modified OM and consequently obtaining the BPCA, 2 mL of nitric acid were added and the samples were digested at 165 ± 5 °C for 8 h. In 2.5 mL aliquots, 50 μL of the internal standards were added: phytalic and citric acids (1 mg mL^{-1}), for correcting from losses during the cleaning procedure. For purification, the samples were placed in columns with cation exchange resins after conditioning (Dowex 50 WX 8, 200-400 mesh, Fluka, Steiheim, Germany). The eluted volume was separated into 4 vials and freeze-dried to be resuspended with methanol and dried with N_2 . To finish “cleaning” the samples, 4 mL of pyridine were added, then the samples were centrifuged and dried once more using N_2 . The internal standard biphenyl-2,2'-dicarboxylic acid was added before derivatization of the samples and the BPCA was quantified from its area. The samples were analyzed with gas chromatography (GC/MS) and liquid chromatography (HPLC). For GC/MS analysis, the samples were derivatized with 250 μL of pyridine and 250 μL of BDTFA + TMS with heating for 2 h at 80 °C for subsequent injection into the gas chromatography apparatus with different detectors (GC/FID, GC/MS). For HPLC analysis, after dried with N_2 , the samples were resuspended with an aqueous phase

consisting of a tetrabutylammonium bromide solution (4 mM, ACS quality) in phosphate buffer (Na_2HPO_4 and NaH_2PO_4 each 5 mM in ultrapure water, pH 7.2). To allow comparisons of the data obtained from the different equipment, the correction factor of 1.5 suggested by Schneider et al. (2011) was used. To attribute accuracy and precision to the analysis, the standard reference sediment NIST 1941b was used in the determination of the BPCA. The mean BC content normalized by the OC content detected by the GC/MS was $2.08 \pm 0.17 \text{ mg g}^{-1} \text{ OC}$ and for HPLC $2.97 \pm 0.26 \text{ mg g}^{-1} \text{ OC}$. The BC content was estimated by the sum of pentacarboxylic (B5CA) and mellitic (B6CA) acids after oxidation with nitric acid. The other groups B3CA and B4CA were not used due to the results observed by Kappenberg et al. (2016), where those two groups were produced after oxidation of non-pyrogenic OM even with low sample weight ($< 5 \text{ mg OC}$).

Sources of organic matter in coastal sediments

Bayesian mixing models can provide a synthesis of source and mixture data into a model structure that incorporates the variability of the data (e.g. isotopic fractionation factor) (Parnell et al., 2010) while linear mixing models consider that diagenetic changes do not change significantly the $\delta^{13}\text{C}$ and $\delta^{15}\text{N}$ values of the OM. Hence, the Bayesian MixSIAR mixing model was used to estimate the contributions of the sources in the sample sets (Stock and Semmens, 2016). The MixSIAR uses Bayesian isotopic mixing and fitting models with Markov chain Monte Carlo (MCMC) simulations of plausible values that are consistent with the dataset ($n = 1,000,000, 100,000, \text{ and } 1,000,000$ for Sinnamary, Amazonas, and PSR coastal zones, respectively). The isotopic fractionation factors used were calculated for each area and each possible source (Supplementary Table 2).

Since it is not possible to access the estimative for each sample through the Bayesian models, to evaluate the contribution of the common terrestrial source (terrestrial C_3 plants) for the samples, the two-end-members (Equation 1) (Schultz and Calder, 1976) and three-end-members model (Equation 2) (Fry, 2013) were used:

$$\text{Eq. 1: } \text{C}_3 \text{ plants} = \left(\frac{\delta^{13}\text{C}_{\text{Marine}} - \delta^{13}\text{C}_{\text{Sample}}}{\delta^{13}\text{C}_{\text{Marine}} - \delta^{13}\text{C}_{\text{Terrestrial}}} \right) \cdot 100$$

Where $\delta^{13}\text{C}_{\text{Sample}}$ is equivalent to the value found for a given sample, and $\delta^{13}\text{C}_{\text{Terrestrial}}$ and $\delta^{13}\text{C}_{\text{Marine}}$ are the values of the isotopic compositions of the terrestrial and marine sources, respectively. The assumed value for the terrestrial C_3 plants end-member was -31.8‰ (Martinelli et al., 2021) and -19.9‰ for the marine end-member (Bianchi et al., 2018). Since the possible OM sources for Sinnamary and PSR coastal zones are different, it was necessary to use the model with the respective $\delta^{13}\text{C}$ and $\delta^{15}\text{N}$ values for each area on the following equation (2):

$$\text{Eq. 2: } \text{C}_3 \text{ plants} = \frac{(\delta^{15}\text{N}_{\text{C}} - \delta^{15}\text{N}_{\text{B}}) \cdot (\delta^{13}\text{C}_{\text{Sample}} - \delta^{13}\text{C}_{\text{B}}) - (\delta^{13}\text{C}_{\text{C}} - \delta^{13}\text{C}_{\text{B}}) \cdot (\delta^{15}\text{N}_{\text{Sample}} - \delta^{15}\text{N}_{\text{B}})}{(\delta^{15}\text{N}_{\text{C}} - \delta^{15}\text{N}_{\text{B}}) \cdot (\delta^{13}\text{C}_{\text{A}} - \delta^{13}\text{C}_{\text{B}}) - (\delta^{13}\text{C}_{\text{C}} - \delta^{13}\text{C}_{\text{B}}) \cdot (\delta^{15}\text{N}_{\text{A}} - \delta^{15}\text{N}_{\text{B}})}$$

Where $\delta^{13}\text{C}_{\text{Sample}}$ and $\delta^{15}\text{N}_{\text{Sample}}$ are the values of the isotopic compositions of the sediment samples. For Sinnamary coastal zone, A, B, and C represent the sources of OM from the terrestrial C_3 plants (mangrove), microphytobenthos (MPB), and marine phytoplankton, respectively. The $\delta^{13}\text{C}$ and $\delta^{15}\text{N}$ values for the mangrove (*Avicennia germinans* litter) were assumed to be -30.1‰ and 2.6‰ for $\delta^{13}\text{C}$ and $\delta^{15}\text{N}$, respectively, and for MPB, the values were -20.9‰ and 4.6‰ (Ray et al., 2018). The marine source values were -23.9‰ and 3.4‰ for $\delta^{13}\text{C}$ and $\delta^{15}\text{N}$, respectively (Matos et al., 2020). Toward the PSR coastal zone, the isotopic compositions of A, B, and C represent the sources: terrestrial C_3 plants, marine phytoplankton, and terrestrial C_4 plants, respectively. The $\delta^{13}\text{C}$ and $\delta^{15}\text{N}$ values for the terrestrial C_3 plant source were -31.3‰ and 2.7‰ , respectively (Martinelli et al., 2021). For marine phytoplankton, the $\delta^{13}\text{C}$ and $\delta^{15}\text{N}$ values were -19.0‰ and 7.5‰ (Gatts et al., 2020), respectively. The isotopic composition values of C and N for terrestrial C_4 plants were -14.6‰ (Ribas, 2012) and 7.1‰ (internal unpublished data), respectively.

Burial Flux

To estimate the burial flux (F_{burial}) of BC in coastal zones sedimentary compartments the following equation (3) was used (Sánchez-García et al., 2013):

$$\text{Eq. 3: } F_{\text{burial}} = \text{BC} \cdot \text{DBD} \cdot \text{SAR} \cdot (1 - \Phi)$$

Where BC is the sum of B5CA and B6CA ($\mu\text{g g}^{-1}$), DBD is the dry bulk density (g cm^{-3}) and SAR is the sedimentation accumulation rate (cm yr^{-1}). The DBD values were calculated for each sample. SAR values were 1 (Marchand, 2017), 1.5 (Matos et al., 2020), and 0.6 (Wanderley et al., 2014) for the Sinnamary River, Amazon, and PSR coastal zones, respectively. The central porosity value (0.75) commonly applied for global calculations was used (Jönsson et al., 2003).

Statistical Analyses

Statistical analyses were performed with R software (R Core Team, 2018). The descriptive statistics used were median and interquartile ranges. Differences in $\delta^{13}\text{C}$ (‰), BC (mg g^{-1} OC), and B6CA:B5CA values between coastal zones were evaluated by ANOVA (*aov*, Base Package, R Core Team, 2018) followed by a multiple comparison test (*TukeyHSD*, base package, R Core Team, 2018), assuming a 95 % confidence level. Pearson's correlation analysis was performed to evaluate the correlation between the parameters (Electrical conductivity, $\delta^{13}\text{C}$, BC, and the estimated sources for OM).

Linear regression models were proposed to evaluate the relationship and behavior between $\delta^{13}\text{C}$, BC and the condensation degree along the electrical conductivity gradient, which, in turn, was used as a tracer of seawater intrusion (*lm*, *ggplot2* Package, R Core Team, 2018). Additionally, to evaluate the sources for BC content, a linear model was constructed between BC and the contribution of terrestrial C_3 plants (*lm*, *ggplot2* Package, R Core Team, 2018). The assumptions of the linear models (normality, linearity, and homoscedasticity of the residuals) were evaluated using a maximum likelihood function (*boxcox*, MASS package, Venables and Ripley, 2002).

RESULTS

Sources of organic matter in coastal sediments

The $\delta^{13}\text{C}$ values of OM from the coastal zone of the PSR were more ^{13}C -enriched (-22.6 ± 1.3 ‰, one-way ANOVA: $F = 6.466$, $p < 0.01$) when compared to those found in the sedimentary compartments of the Sinnamary and Amazon River coastal zones (-25.0 ± 3.1 and -26.1 ± 1.0 ‰, respectively) (Figure 2A; Supplementary Table 2). Along the electrical conductivity gradient, $\delta^{13}\text{C}$ values of OM ranged between -27.7 and -25.1 ‰, -32.4 and -20.7 ‰, and -24.8 and -20.4 ‰ for the Sinnamary, Amazon, and PSR coastal zones, respectively, with a tendency towards ^{13}C enrichment with increasing electrical conductivity values (Figure 2B).

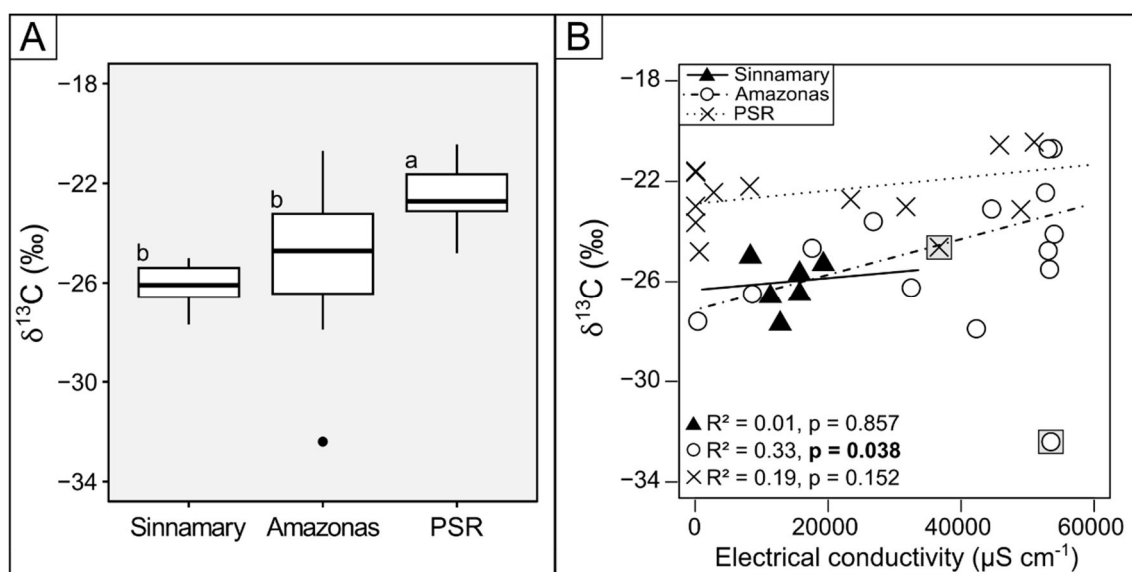


Figure 2. Boxplot representation of $\delta^{13}\text{C}$ values (A) and their distribution along the electrical conductivity gradient for the Sinnamary, Amazon, and PSR coastal zones (B). Different letters upon the boxplots represent statistical support for the difference of the mean (Tukey's test, $p < 0.05$) and circles represent outliers (A). Linear regressions of the models were $Y = -26.48 + 0.00002 X$, $Y = -27.14 + 0.00007 X$, and $Y = -22.89 + 0.00002 X$ for the Sinnamary, Amazon, and PSR coastal zones, respectively (B). The highlighted symbols were not used in the construction of the models.

The composition of sources of sedimentary organic matter was modeled by the Bayesian stable isotope mixing models. The estimated relative percentages of sources contributing to OM for the Sinnamary River coastal sediments averaged 35, 27, and 37 % for marine sources, MPB, and terrestrial C_3 plants, respectively. For the Amazon coastal sediments, C_3 plants accounted for 49 % of the OM. The contributions for the PSR coastal sediments were 41 % for marine sources, 35 % for C_3 plants, and 24 % for C_4 plants.

BC in coastal zones

The BC content, normalized by OC content, showed similar distribution among the three coastal zones (one-way ANOVA: $F = 2.598$, $p = 0.095$) (Figure 3A). The OC content for the Sinnamary, Amazon, and PSR coastal zones were 0.73 ± 0.68 , 0.32 ± 0.24 , and 0.95 ± 0.74 mg g⁻¹ OC, respectively (Figure 3A; Supplementary Table 2). When considering the electrical conductivity gradient, the BC content showed different distribution for the zones (Figure 3C). For the PSR coastal zone, the content tended to increase with increasing electrical conductivity values, while there was a rapid decrease in content for the Sinnamary coastal zone and little variation in the Amazon coastal zone (Figure 3C). The B6CA:B5CA ratio, used to evaluate the degree of condensation of BC, was higher for the PSR coastal zone sample set (one-way ANOVA: $F = 4.826$, $p < 0.05$) (Figure 3B). The degree of condensation for the Sinnamary, Amazon, and PSR was 0.28 ± 0.17 , 0.29 ± 0.23 , and 0.50 ± 0.15 , respectively (Figure 3B). Similar to BC content, the degree of condensation was different along the electrical conductivity gradient for the coastal zones (Figure 3D). A rapid decrease in the degree of condensation was observed in the Sinnamary coastal zone, while an increase was observed in the Amazon coastal zone and little variation took place in the PSR coastal zone (Figure 3D).

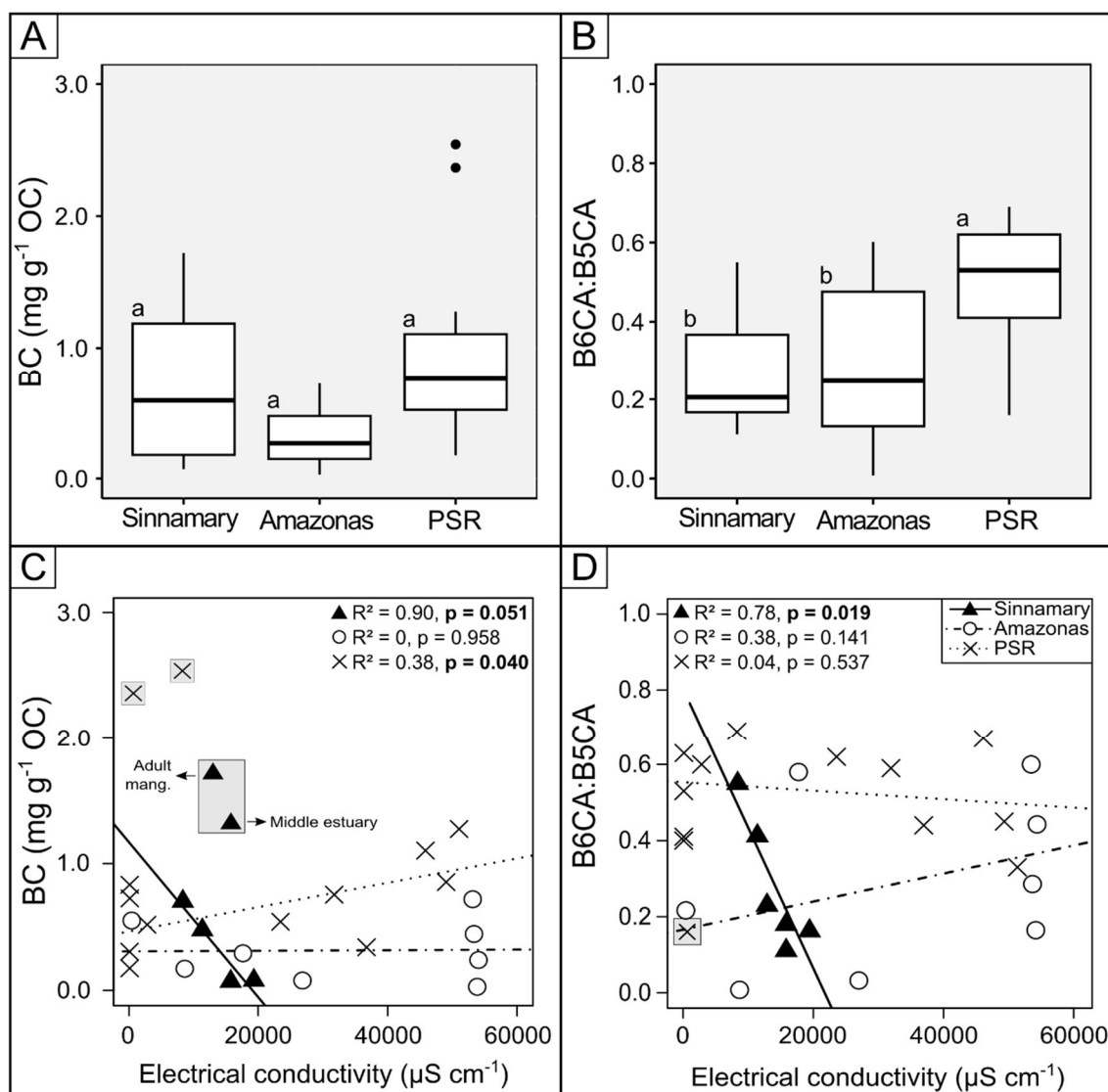


Figure 3. Boxplot representation of BC values normalized by OC content (A) and degree of condensation (B). BC content (C) and degree of condensation (D) along the electrical conductivity gradient in the coastal areas of the Sinnamary, the Amazon, and the PSR. Different letters upon the boxplots represent statistical support for the difference of the mean (Tukey's test, $p < 0.05$) and circles represent outliers (A and B). The linear regressions of the models for BC were $Y = 1.17 - 0.00006 X$, $Y = 0.31 + 0.0000002 X$, and $Y = 0.47 + 0.00001 X$ for the Sinnamary, Amazon and PSR coastal zones, respectively (C). Models of the degree of condensation were constructed from the equations: $Y = 0.81 - 0.00004 X$, $Y = 0.05 + 0.0000056 X$, and $Y = 0.55 - 0.000001 X$ for the Sinnamary, Amazon, and PSR coastal zones, respectively (D). The highlighted symbols were not used in the construction of the models.

DISCUSSION

Sources of organic matter in coastal sediments

The ^{13}C enrichment of the PSR coastal zone represents a typical signal of terrestrial C_3 - C_4 plants mixtures, showing changes in land use in this drainage basin reflecting surface sediments. In the Amazon and Sinnamary, the sedimentary OM has a strong signal from C_3 plants from the local forests (Figure 2A). However, the enrichment of ^{13}C values in the coastal zone sediments indicates a contribution of the marine source for sedimentary OM with increasing electrical conductivity values for the Amazon and PSR (Figure 2B). When evaluating the particulate OC along the continent – ocean gradient of the PSR, Marques (2017) observed ^{13}C -enriched values ranging from -25 to -23 ‰, with C_4 plant contribution ranging from 27 to 40 %. In addition, according to the same author, the variation in $\delta^{13}\text{C}$ values in the estuarine samples depends on river discharge, as in events of higher river discharge the author found more ^{13}C depleted values, indicating a stronger contribution from mangroves (terrestrial C_3 plants) present in the estuarine zone during high flow.

By using coupled $\delta^{13}\text{C}$ values with the atomic ratio between carbon and nitrogen $[(\text{C}:\text{N})_a]$ and with $\delta^{15}\text{N}$ it is possible to distinguish the proportions of possible OM sources for the sediment samples (Figure 4). There is heterogeneous variation in the sources contributing to the OM of coastal zone surface sediments, with marine sources contributing intensely to some samples from the PSR and the Amazon coastal zones (Figure 4A). According to Ward et al. (2015), about 50 % of continental OM does not reach the coastal zone due to a combination of intense remineralization and the OM sedimentation processes occurring in the Amazon River. In the Amazon River plume, OM continues to be extensively remineralized and terrestrial OM is rapidly replaced by marine OM, which explains the strong enrichment in ^{13}C along the conductivity gradient (Aller and Blair, 2006) (Figure 2B). The relationship between the OM tracers shows that the samples from the Sinnamary coastal zone have a majority contribution of C_3 vegetation, probably a mixture of the mangrove present in the estuary, vegetation debris transported by the river, and freshwater phytoplankton (Figure 4B). When investigating the SPM in the Sinnamary estuary, Ray et al. (2018) observed the same sources for OM and also reported the important contribution of biofilm formed by MPB to the sediment compartment.

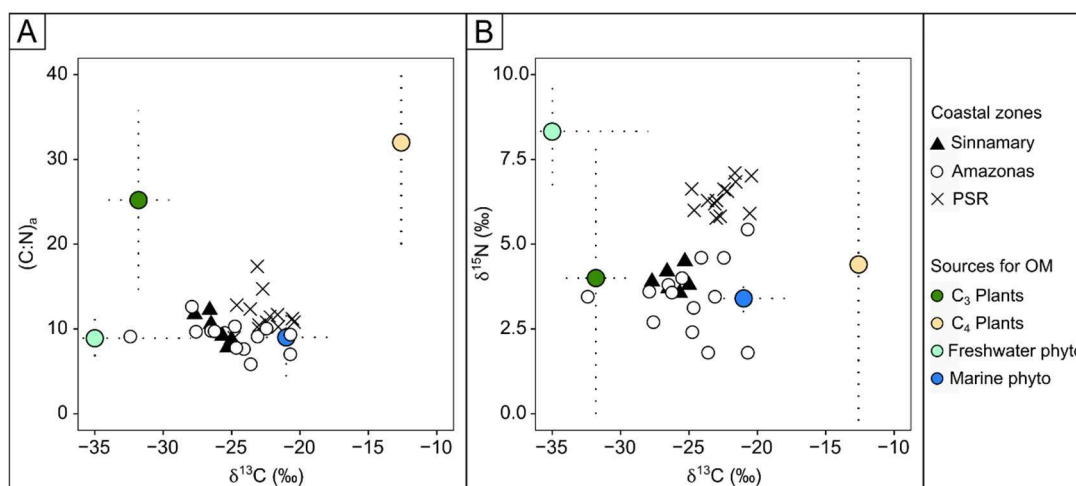


Figure 4. $\delta^{13}\text{C}$ vs. $(\text{C:N})_a$ (A) and $\delta^{13}\text{C}$ vs. $\delta^{15}\text{N}$ (B) in the coastal zones of the Sinnamary, Amazon, and PSR. End Members sources from Martinelli et al. (2021), Hamilton and Lewis (1992), Bouillon et al. (2011), Ribas (2012), Ellis et al. (2012) and Caraballo et al. (2014) and Ray et al. (2018).

The MixSIAR modeling showed the contribution of potential sources to the OC content in the three coastal zones. Sinnamary coastal zone samples set showed the majority contribution from terrestrial C₃ plants, except for the sample collected near the mangrove pioneer area, in which 55 % of OM sediment was from MPB. Conversely, the surface sediment sample collected in the adult mangrove area showed the lowest contribution of MPB (19 %) and the highest contribution of terrestrial C₃ plants, around 70 %, among the samples collected in the coastal zone of the Sinnamary River. According to Marchand et al. (2003), the decrease in the presence of biofilm formed by MPB occurs with increasing mangrove age, and this explains the strong negative correlation observed between the contributions of terrestrial C₃ plants and MPB to the OC content of the Sinnamary estuary sediment in the present study ($r = -0.92$, $p = 0.009$). The high marine source contribution to the PSR coastal sediments can be attributed to the low discharge of the PSR observed during the sampling period, as a consequence of low precipitation (below 50 % of normal) observed as a result of the La Niña macroclimatic variation (Marques et al., 2017; Costa et al., 2018), and also due to anthropic modifications of the PSR watershed (Carvalho et al., 2002; Souza et al., 2010). A majority of the marine source was also observed on the Amazon samples, the same trend observed by Sun et al. (2017), with $\delta^{13}\text{C}$ values enriched in ¹³C (-18.6 ‰) on the marine surface sediments. Additionally, by analyzing the phenolic products of lignin, the authors also observed that terrestrial OM reaching the area of influence of the

Amazon River plume undergoes extensive diagenetic alteration before it is deposited, as previously observed by Aller and Blair (2006) and Ward et al. (2015).

BC in coastal zones

No statistical differences were observed between the BC content found in the different coastal zones, even though the divergence between the sizes of drainage basins and river discharge (Figure 1, 3A). Similarly, Coppola et al. (2018) also did not observe a statistical difference in the BC contribution to the OC content between the largest rivers worldwide and small rivers. However, the measure of central tendency was relatively lower in the Amazon coastal zone when compared to the Sinnamary and PSR coastal zones. The same trend was observed by Coppola et al. (2018), where BC content contributed to around 14 % of the OC on the largest rivers, and around 18 % for small rivers. The relatively low BC content observed in the coastal zone of the Amazon River can initially be explained by dilution caused by high river discharge (Figure 3A). In addition, the high residence time of particles in river systems with extensive lowlands results in higher remineralization of OM transported along with the river system (Bianchi et al., 2018). As consequence, the BC mainly composed of labile and semi-labile carbon can be degraded and replaced by non-thermally modified OM in floodplains before reaching the coastal zone (Frueh and Lancaster, 2014; Cotrufo et al., 2016). This likely degradation in the fluvial section of the continent – ocean gradient explains not only the low content but also the low variation observed along the electrical conductivity gradient, indicating that the pyrogenic material found in the coastal zone of the Amazon may be composed mainly of stable polycyclic aromatic carbon (Figure 3A and C) (Bird et al., 2015). The heterogeneity in the degree of condensation of the samples along the electrical conductivity gradient indicates that there may be at least two mechanisms acting on the deposition of BC in the sedimentary compartment: the removal of hydrophobic components from the dissolved BC fraction followed by co-precipitation (Coppola et al., 2014), and remobilization of aged BC from alluvial sedimentary deposits (Wagner et al., 2018). On the North Pacific Ocean, in addition to photodegradation controlling the loss of BC in the dissolved fraction of water, adsorption of the highly condensed structures onto particles has also been shown to be an important removal mechanism of BC in marine systems (Nakane et al., 2017). Due to the

energetic margin and high loading of the Amazon River, particles are subject to numerous cycles of deposition and resuspension during lateral transport and, as a consequence, BC can be stocked in intermediate reservoirs before composing the marine sediment compartment (McKee et al., 2004; Coppola et al., 2018). The heterogeneity trend for the degree of condensation found by Sánchez-García et al. (2013) in coastal sediments on the Guadiana plume, also indicated the fluvial transport of aged BC near the coast as an important process for BC deposition in the coastal sediment. Thus, it can be inferred that samples with a low degree of condensation may reflect aged condensed compounds due to intense remineralization along the entire Amazon gradient (Coppola et al., 2014).

Although the measure of central tendency for BC content in sediments from the coastal zones of the Sinnamary River and PSR were similar, they showed different trends along the electrical conductivity gradient (Figure 3A and B). In contrast to the transport of BC along the continent – ocean gradient in the Amazon River, in small to medium-sized rivers, such as the Sinnamary and PSR Rivers, BC reaches the coastal zone more rapidly due to the relatively short time between entry into the aquatic environment and deposition in coastal sediments (Burdige, 2007). In Sinnamary coastal zone, BC appears to be rapidly degraded along the electrical conductivity gradient. Although dilution by SPM transported by the Amazon River plume into the coastal zone of French Guiana seems to explain the low concentrations of inorganic pollutants in the sediment of Sinnamary estuary (Marchand et al., 2006), the decrease in BC content seems to be driven by the dominance of labile and semi-labile aromatic carbon, a trend consistent with the observed decrease in the degree of BC condensation. Unlike stable polycyclic aromatic carbon that can persist in environmental compartments for hundreds of years, the labile and semi-labile components of BC can be remineralized or transformed over timescales of a few years to a few decades (Bird et al., 2015). The highest BC content observed for this zone was in sediments in an adult mangrove channel and the salt wedge. Mangroves have a large capacity to retain allochthonous OM in their sediment compartment from fluvial transport (Chew and Gallagher, 2018). When evaluating the proportion of BC to OC sediment content in mangroves, Chew and Gallagher (2018) found high contributions of BC to OC content and attributed the high concentration to fluvial transport, since mangroves do not burn. Moreover, it is important to emphasize the importance of BC trapping

from soot through the canopy (Agawin and Duarte, 2002). In the salt wedge zone, flocculation and subsequent deposition can facilitate the accumulation of fine particles becoming a site of thermally and non-thermally modified OM deposition (Eisma et al., 1994).

Along the electrical conductivity gradient of the PSR coastal zone, the increased content and stability of the degree of BC condensation highlights the refractory nature of BC for this coastal region. Saiz et al. (2015) observed that in landscapes consisting mainly of grasses, higher production of stable material is observed. Thus, the current BC production in the PSR basin seems to explain the higher degree of BC condensation of the zone and the stability of the thermally modified OM along the electrical conductivity gradient. By using the relation between BC and the contribution of terrestrial C₄ plant, Marques et al. (2017) identified the historical burning of the Atlantic rainforest as the predominant source of dissolved BC in the PSR, as previously suggested by Dittmar et al. (2012), with the degree of condensation ranging between 0.27 and 0.38. The solubilization of BC in soil and its subsequent entry into the aquatic system can take hundreds of years, which seems to explain the results found by the authors. Thus, it is expected that BC from historical burning is removed from soil mainly by the solubilization of soil OM (Dittmar et al., 2012). Changes in vegetation cover and current BC production increase soil erosion (Smith et al., 2011) making the input of recently produced BC into the aquatic system more important for the SPM. When estimating BC content in the particulate and dissolved fractions of water, Wagner et al. (2015) observed an immediate contribution of BC after combustion to the SPM with a decrease each year following the burning event. However, management by fire in pasture and sugarcane areas continues to occur annually in the PSR basin (Ferreira et al., 2021), thereby increasing the pool of BC in soils. Thus, the difference in source and quality between BC in the sediment compartment in the present study and the dissolved fraction (Marques et al., 2017) can be explained by differences in molecular composition modulation for the different water fractions (Wagner et al., 2018).

Sources for BC and burial flux

From the relationship between the contribution of C₃ plants to sedimentary OM and the BC content found from coastal zones, it was possible to infer that the

thermally modified OM of the sediment compartment of each zone tends to vary with the current vegetation cover of each basin (Figure 5). The estimated C_3 plants' contribution does not distinguish vascular plants from the autochthonous production on the rivers, thereby, the determination coefficient exhibited this "mixture" factor. Although the history of Atlantic rainforest burning explains the BC concentrations in the dissolved fraction of water (Marques et al., 2017), the BC content in sediments tends to decrease with increasing terrestrial C_3 source contribution to the OM of the PSR coastal sediment. High BC content ($2.37 \text{ mg g}^{-1} \text{ OC}$) found in a sample where there is no contribution from terrestrial C_4 plants and exhibiting a low degree of condensation may indicate the contribution of old BC from historical burning. Jones et al. (2017) highlight the importance of atmospheric soot deposition for the BC content in the PSR, as recently produced soot (e.g., from biomass or fossil fuel burning) that is not transferred to BC in the dissolved fraction can be transported with the SPM along the river and be deposited. Thus, in addition to being carried via river transport, some of the BC deposited in the coastal zone of the PSR can be transported via the atmosphere. Atmospheric transport into the coastal zones of the Amazon and Sinnamary Rivers does not appear to be important for BC content. According to Coppola et al. (2019), BC from atmospheric deposition is rapidly removed or diluted in the fluvial sector of the Amazon River.

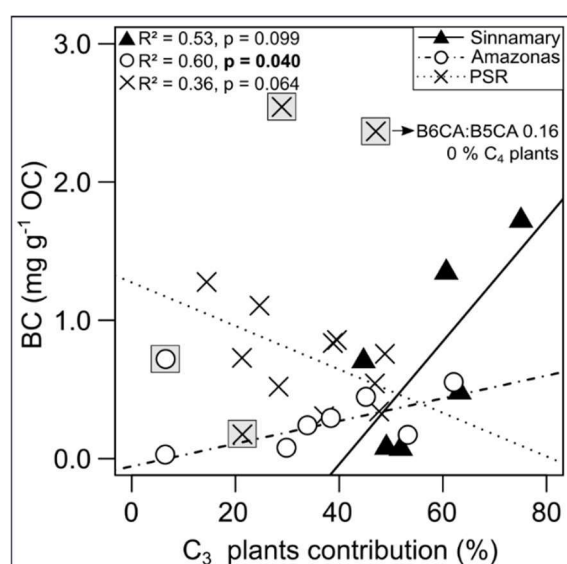


Figure 5. Contribution of terrestrial C_3 plant for the OM vs. BC content to the coastal zones of the Sinnamary, Amazon, and PSR. The linear regressions of the models were $Y = -1.818 + 0.004 X$, $Y = -0.056 + 0.008 X$, and $Y = 1.274 - 0.016 X$ for the Sinnamary, Amazon, and PSR coastal zones, respectively. The highlighted symbols were not used in the construction of the models.

Estimates of burial flux for coastal zones are important for better understanding the global budgets of thermally modified OM in coastal sediments since it is their final fate (Sánchez-García et al., 2013). The burial flux of BC content was calculated for the coastal zones and showed mean values of 1.5 ± 1.5 , 0.5 ± 0.4 , and $2.4 \pm 1.5 \mu\text{g cm}^{-2} \text{y}^{-1}$ for the coastal zones of the Sinnamary, Amazon, and PSR Rivers, respectively. Receiving a constant input of BC from the management of cropland and pasture areas that constitute the landscape of the devastated biome, the PSR coastal zone showed a higher burial flux of BC among the study areas. Since there are different techniques for determining BC in different areas of the combustion continuum and different uses of the same technique (e.g., using B3CA and B4CA acids in estimating BC content and/or applying conversion factors [Glaser et al., 1998]), comparisons between different investigations based on different methodologies and data analysis techniques should be performed with caution.

CONCLUSION

By coupling the $\delta^{13}\text{C}$ with other OM tracers ($\delta^{15}\text{N}$ and $(\text{C:N})_a$) data, it was possible to understand the dynamics of the OM of the coastal zones and estimate the contributions of the sources from the Bayesian model, MixSiar. Also, it made it possible to evaluate if the modification of the vegetation cover of the PSR basin from forest to grass had modified the quality of the OM transported to the coastal ocean. Additionally, we combined the common terrestrial source contribution (terrestrial C_3 plants) and BC content to understand BC production in the drainage basins of the coastal areas of the present study.

PSR set samples exhibited values of the mixture of C_3 and C_4 plants, with more ^{13}C -enriched values, showing that the modification of the Atlantic Rainforest to cropland and pasture areas is changing the OM associated with the particles transported to the coastal zone. Even though the $\delta^{13}\text{C}$ analysis was performed on the OC bulk and not on the molecular markers of BC – the BPCA, it is possible to assume that the BC production from the incomplete burning of terrestrial C_4 plant biomass is the main source of BC on the PSR coastal sediments.

The processes that SPM is subject to in the fluvial portion of the Amazon River and the dilution by high material discharge guide the low black carbon content in the coastal zone, but this may change due to the high degree of agricultural speculation in the Amazon fostered by current Brazilian government policies will exacerbate both, social and ecological impacts on the biome. Over the last 14 years, deforestation and forest fire rates in Brazil's Legal Amazon have increased to record levels. Thus, fires from anthropic activities that increasingly remove biomass in the Amazon rainforest can increase the content of BC transported to the coastal zone. Even though the land-use change exhibited a potential to produce more BC dominated by stable aromatic carbon in this study, it is important to consider that the Amazon Rainforest accounts for 93 ± 23 Pg C aboveground, which can substantially increase BC production and have significant impacts on the carbon cycle.

REFERENCES

- Agawin, N.S.R., Duarte, C.M., 2002. Evidence of direct particle trapping by a tropical seagrass meadow. *Estuaries*. <https://doi.org/10.1007/bf02692217>
- Aller, R.C., 1998. Mobile deltaic and continental shelf muds as suboxic, fluidized bed reactors. *Marine Chemistry*. [https://doi.org/10.1016/s0304-4203\(98\)00024-3](https://doi.org/10.1016/s0304-4203(98)00024-3)
- Aller, R.C., Blair, N.E., 2006. Carbon remineralization in the Amazon–Guianas tropical mobile mudbelt: A sedimentary incinerator. *Continental Shelf Research*. <https://doi.org/10.1016/j.csr.2006.07.016>
- Aller, R.C., Blair, N.E., Xia, Q., Rude, P.D., 1996. Remineralization rates, recycling, and storage of carbon in Amazon shelf sediments. *Continental Shelf Research*. [https://doi.org/10.1016/0278-4343\(95\)00046-1](https://doi.org/10.1016/0278-4343(95)00046-1)
- Aller, R.C., Heilbrun, C., Panzeca, C., Zhu, Z., Baltzer, F., 2004. Coupling between sedimentary dynamics, early diagenetic processes, and biogeochemical cycling in the Amazon–Guianas mobile mud belt: coastal French Guiana. *Marine Geology*. <https://doi.org/10.1016/j.margeo.2004.04.027>
- Allison, M.A., Lee, M.T., 2004. Sediment exchange between Amazon mudbanks and shore-fringing mangroves in French Guiana. *Marine Geology*. <https://doi.org/10.1016/j.margeo.2004.04.026>

- Aragão, L.E.O.C., Anderson, L.O., Fonseca, M.G., Rosan, T.M., Vedovato, L.B., Wagner, F.H., Silva, C.V.J., Silva Junior, C.H.L., Arai, E., Aguiar, A.P., Barlow, J., Berenguer, E., Deeter, M.N., Domingues, L.G., Gatti, L., Gloor, M., Malhi, Y., Marengo, J.A., Miller, J.B., Phillips, O.L., Saatchi, S., 2018. 21st Century drought-related fires counteract the decline of Amazon deforestation carbon emissions. *Nature Communication*. <https://doi.org/10.1038/s41467-017-02771-y>
- Assis, L. F. F. G.; Ferreira, K. R.; Vinhas, L.; Maurano, L.; Almeida, C.; Carvalho, A.; Rodrigues, J.; Maciel, A.; Camargo, C., 2019. TerraBrasilis: A Spatial Data Analytics Infrastructure for Large-Scale Thematic Mapping. *ISPRS International Journal of Geo-Information*. <https://doi.org/10.3390/ijgi8110513>
- Bernardes, M.C., Martinelli, L.A., Krusche, A.V., Gudeman, J., Moreira, M., Victoria, R.L., Ometto, J.P.H., Ballester, M.V.R., Aufdenkampe, A.K., Richey, J.E., Hedges, J.I., 2004. Riverine organic matter composition as a function of land use change, Southwest Amazon. *Ecological Applications*. <https://doi.org/10.1890/01-6028>
- Bernini, E., Rezende, C.E., 2004. Estrutura da vegetação em florestas de mangue do estuário do rio Paraíba do Sul, Estado do Rio de Janeiro, Brasil. *Acta Botanica Brasilica*. <https://doi.org/10.1590/s0102-33062004000300009>
- Bianchi, T.S., Cui, X., Blair, N.E., Burdige, D.J., Eglinton, T.I., Galy, V., 2018. Centers of organic carbon burial and oxidation at the land-ocean interface. *Organic Geochemistry*. <https://doi.org/10.1016/j.orggeochem.2017.09.008>
- Bird, M.I., Ascough, P.L., 2012. Isotopes in pyrogenic carbon: A review. *Organic Geochemistry*. <https://doi.org/10.1016/j.orggeochem.2010.09.005>
- Bird, M.I., Wynn, J.G., Saiz, G., Wurster, C.M., McBeath, A., 2015. The Pyrogenic Carbon Cycle. *Annual Review of Earth and Planetary Sciences*. <https://doi.org/10.1146/annurev-earth-060614-105038>
- Blair, N.E., Leithold, E.L., Ford, S.T., Peeler, K.A., Holmes, J.C., Perkey, D.W., 2003. The persistence of memory: the fate of ancient sedimentary organic carbon in a modern sedimentary system. *Geochimica et Cosmochimica Acta*. [https://doi.org/10.1016/s0016-7037\(02\)01043-8](https://doi.org/10.1016/s0016-7037(02)01043-8)
- Bouillon, S., Connolly, R.M., Gillikin, D.P., 2011. Use of Stable Isotopes to Understand Food Webs and Ecosystem Functioning in Estuaries. *Treatise*

- on Estuarine and Coastal Science. <https://doi.org/10.1016/b978-0-12-374711-2.00711-7>
- Brodowski, S., Rodionov, A., Haumaier, L., Glaser, B., Amelung, W., 2005. Revised black carbon assessment using benzene polycarboxylic acids. *Organic Geochemistry*. <https://doi.org/10.1016/j.orggeochem.2005.03.011>
- Burdige, D.J., 2007. Preservation of Organic Matter in Marine Sediments: Controls, Mechanisms, and an Imbalance in Sediment Organic Carbon Budgets? *ChemInform*. <https://doi.org/10.1002/chin.200720266>
- Cai, D.-L., Tan, F.C., Edmond, J.M., 1988. Sources and transport of particulate organic carbon in the Amazon River and estuary. *Estuarine, Coastal and Shelf Science*. [https://doi.org/10.1016/0272-7714\(88\)90008-x](https://doi.org/10.1016/0272-7714(88)90008-x)
- Caraballo, P., Forsberg, B.R., de Almeida, F.F., Leite, R.G., 2014. Diel patterns of temperature, conductivity and dissolved oxygen in an Amazon floodplain lake: description of a fríagem phenomenon. *Acta Limnologica Brasiliensia*. <https://doi.org/10.1590/s2179-975x2014000300011>
- Carvalho, C.E.V., Salomão, M.S.M., Molisani, M.M., Rezende, C.E., Lacerda, L.D., 2002. Contribution of a medium-sized tropical river to the particulate heavy-metal load for the South Atlantic Ocean. *Science of The Total Environment*. [https://doi.org/10.1016/s0048-9697\(01\)00869-5](https://doi.org/10.1016/s0048-9697(01)00869-5)
- Chave, J., Riéra, B., Dubois, M.-A., 2001. Estimation of biomass in a neotropical forest of French Guiana: spatial and temporal variability. *Journal of Tropical Ecology*. <https://doi.org/10.1017/s0266467401001055>
- Chew, S.T., Gallagher, J.B., 2018. Accounting for black carbon lowers estimates of blue carbon storage services. *Sci. Rep.* 8, 2553. <https://doi.org/10.1038/s41598-018-20644-2>
- Coppola, A.I., Wiedemeier, D.B., Galy, V., Haghypour, N., Hanke, U.M., Nascimento, G.S., Usman, M., Blattmann, T.M., Reisser, M., Freymond, C.V., Zhao, M., Voss, B., Wacker, L., Schefuß, E., Peucker-Ehrenbrink, B., Abiven, S., Schmidt, M.W.I., Eglinton, T.I., 2018. Publisher Correction: Global-scale evidence for the refractory nature of riverine black carbon. *Nature Geoscience*. <https://doi.org/10.1038/s41561-018-0252-z>
- Coppola, A.I., Ziolkowski, L.A., Masiello, C.A., Druffel, E.R.M., 2014. Aged black carbon in marine sediments and sinking particles. *Geophysical Research Letters*. <https://doi.org/10.1002/2013gl059068>

- Costa, L. F., de Farias Júnior, J. E. F., Johnson, R. M. F., Petrunaro, A. C. N., & Ramos, N. P., 2018. Análise da precipitação da bacia do rio Paraíba do Sul com enfoque nos anos de 2014 a 2017.
- Cotrufo, M.F., Francesca Cotrufo, M., Boot, C.M., Kampf, S., Nelson, P.A., Brogan, D.J., Covino, T., Haddix, M.L., MacDonald, L.H., Rathburn, S., Ryan-Bukett, S., Schmeer, S., Hall, E., 2016. Redistribution of pyrogenic carbon from hillslopes to stream corridors following a large montane wildfire. *Global Biogeochemical Cycles*. <https://doi.org/10.1002/2016gb005467>
- Dittmar, T., 2008. The molecular level determination of black carbon in marine dissolved organic matter. *Organic Geochemistry*. <https://doi.org/10.1016/j.orggeochem.2008.01.015>
- Dittmar, T., de Rezende, C.E., Manecki, M., Niggemann, J., Ovalle, A.R.C., Stubbins, A., Bernardes, M.C., 2012. Continuous flux of dissolved black carbon from a vanished tropical forest biome. *Nature Geoscience*. <https://doi.org/10.1038/ngeo1541>
- Edwards, P.J., 1984. *The Use of Fire as a Management Tool*. Ecological Studies. https://doi.org/10.1007/978-3-642-69805-7_16
- Eisma, D., Chen, S., Li, A., 1994. Tidal variations in suspended matter floc size in the Elbe river and Dollard estuaries. *Netherlands Journal of Aquatic Ecology*. <https://doi.org/10.1007/bf02334194>
- Ellis, E.E., Keil, R.G., Ingalls, A.E., Richey, J.E., Alin, S.R., 2012. Seasonal variability in the sources of particulate organic matter of the Mekong River as discerned by elemental and lignin analyses. *Journal of Geophysical Research: Biogeosciences*. <https://doi.org/10.1029/2011jg001816>
- Ferrante, L., Fearnside, P.M., 2019. Brazil's new president and "ruralists" threaten Amazonia's environment, traditional peoples and the global climate. *Environmental Conservation*. <https://doi.org/10.1017/s0376892919000213>
- Ferreira, R., Nunes, C., Souza, M., Canela, M., 2021. Multivariate Optimization of Extraction Variables of PAH in Particulate Matter (PM10) in Indoor/Outdoor Air at Campos dos Goytacazes, Brazil. *Journal of the Brazilian Chemical Society*. <https://doi.org/10.21577/0103-5053.20200216>
- Figueiredo, R. de O., de Oliveira Figueiredo, R., Ovalle, A.R.C., de Rezende, C.E., Martinelli, L.A., 2011. Carbon and Nitrogen in the Lower Basin of the Paraíba do Sul River, Southeastern Brazil: Element fluxes and

- biogeochemical processes. *Ambiente e Agua - An Interdisciplinary Journal of Applied Science*. <https://doi.org/10.4136/ambi-agua.183>
- Forbes, M.S., Raison, R.J., Skjemstad, J.O., 2006. Formation, transformation and transport of black carbon (charcoal) in terrestrial and aquatic ecosystems. *Sci. Total Environ.* 370, 190–206. <https://doi.org/10.1016/j.scitotenv.2006.06.007>
- Fromard, F., Vega, C., Proisy, C., 2004. Half a century of dynamic coastal change affecting mangrove shorelines of French Guiana. A case study based on remote sensing data analyses and field surveys. *Marine Geology*. <https://doi.org/10.1016/j.margeo.2004.04.018>
- Frueh, W.T., Terry Frueh, W., Lancaster, S.T., 2014. Correction of deposit ages for inherited ages of charcoal: implications for sediment dynamics inferred from random sampling of deposits on headwater valley floors. *Quaternary Science Reviews*. <https://doi.org/10.1016/j.quascirev.2013.10.029>
- Fry, B., 2013. Alternative approaches for solving underdetermined isotope mixing problems. *Marine Ecology Progress Series*. <https://doi.org/10.3354/meps10168>
- Gallo, M.N., Vinzon, S.B., 2015. Estudo numérico do escoamento em planícies de marés do canal Norte (estuário do rio Amazonas). *Ribagua*. <https://doi.org/10.1016/j.riba.2015.04.002>
- Gatti, L.V., Basso, L.S., Miller, J.B., Gloor, M., Domingues, L.G., Cassol, H.L.G., Tejada, G., Aragão, L.E.O., Nobre, C., Peters, W., Marani, L., Arai, E., Sanches, A.H., Corrêa, S.M., Anderson, L., Von Randow, C., Correia, C.S.C., Crispim, S.P., Neves, R.A.L., 2021. Amazonia as a carbon source linked to deforestation and climate change. *Nature*. <https://doi.org/10.1038/s41586-021-03629-6>
- Gatts, P.V., Franco, M.A.L., Almeida, M.G., Zalmon, I.R., Di Benedetto, A.P.M., Costa, P.A.S., de Rezende, C.E., 2020. The trophic ecology of marine catfishes in south-eastern Brazil. *Journal of the Marine Biological Association of the United Kingdom*. <https://doi.org/10.1017/s0025315419001164>
- Geyer, W.R., Rockwell Geyer, W., Beardsley, R.C., Lentz, S.J., Candela, J., Limeburner, R., Johns, W.E., Castro, B.M., Soares, I.D., 1996. Physical

- oceanography of the Amazon shelf. *Continental Shelf Research*.
[https://doi.org/10.1016/0278-4343\(95\)00051-8](https://doi.org/10.1016/0278-4343(95)00051-8)
- Glaser, B., Haumaier, L., Guggenberger, G., Zech, W., 1998. Black carbon in soils: the use of benzenecarboxylic acids as specific markers. *Organic Geochemistry*. [https://doi.org/10.1016/s0146-6380\(98\)00194-6](https://doi.org/10.1016/s0146-6380(98)00194-6)
- Goldberg, E.D., 1985. *Black Carbon in the Environment: Properties and Distribution*. Wiley-Interscience.
- Hamilton, S.K., Lewis, W.M., 1992. Stable carbon and nitrogen isotopes in algae and detritus from the Orinoco River floodplain, Venezuela. *Geochimica et Cosmochimica Acta*. [https://doi.org/10.1016/0016-7037\(92\)90264-j](https://doi.org/10.1016/0016-7037(92)90264-j)
- Hedges, J.I., Eglinton, G., Hatcher, P.G., Kirchman, D.L., Arnosti, C., Derenne, S., Evershed, R.P., Kögel-Knabner, I., de Leeuw, J.W., Littke, R., Michaelis, W., Rullkötter, J., 2000. The molecularly-uncharacterized component of nonliving organic matter in natural environments. *Organic Geochemistry*. [https://doi.org/10.1016/s0146-6380\(00\)00096-6](https://doi.org/10.1016/s0146-6380(00)00096-6)
- Jones, M.W., Quine, T.A., de Rezende, C.E., Dittmar, T., Johnson, B., Manecki, M., Marques, J.S.J., de Aragão, L.E.O.C., 2017. Do Regional Aerosols Contribute to the Riverine Export of Dissolved Black Carbon? *Journal of Geophysical Research: Biogeosciences*. <https://doi.org/10.1002/2017jg004126>
- Jönsson, A., Gustafsson, Ö., Axelman, J., Sundberg, H., 2003. Global Accounting of PCBs in the Continental Shelf Sediments. *Environmental Science & Technology*. <https://doi.org/10.1021/es0201404>
- Jurado, E., Dachs, J., Duarte, C.M., Simó, R., 2008. Atmospheric deposition of organic and black carbon to the global oceans. *Atmospheric Environment*. <https://doi.org/10.1016/j.atmosenv.2008.07.029>
- Kuehl, S.A., DeMaster, D.J., Nittrouer, C.A., 1986. Nature of sediment accumulation on the Amazon continental shelf. *Continental Shelf Research*. [https://doi.org/10.1016/0278-4343\(86\)90061-0](https://doi.org/10.1016/0278-4343(86)90061-0)
- Kuhlbusch, T.A.J., Crutzen, P.J., 1995. Toward a global estimate of black carbon in residues of vegetation fires representing a sink of atmospheric CO₂ and a source of O₂. *Global Biogeochemical Cycles*. <https://doi.org/10.1029/95gb02742>

- Latrubesse, E.M., 2008. Patterns of anabranching channels: The ultimate end-member adjustment of mega rivers. *Geomorphology*. <https://doi.org/10.1016/j.geomorph.2008.05.035>
- Laurance, W.F., Albernaz, A.K.M., Da Costa, C., 2001. Is deforestation accelerating in the Brazilian Amazon? *Environmental Conservation*. <https://doi.org/10.1017/s0376892901000339>
- Luglia, M., Criquet, S., Sarrazin, M., Guiral, D., 2019. Extracellular enzyme activities of estuarine mudflats in French Guiana in relation with environmental factors across spatial and seasonal scales. *Estuarine, Coastal and Shelf Science*. <https://doi.org/10.1016/j.ecss.2019.106243>
- Major, J., Lehmann, J., Rondon, M., Goodale, C., 2010. Fate of soil-applied black carbon: downward migration, leaching and soil respiration. *Global Change Biology*. <https://doi.org/10.1111/j.1365-2486.2009.02044.x>
- Malhi, Y., Roberts, J.T., Betts, R.A., Killeen, T.J., Li, W., Nobre, C.A., 2008. Climate change, deforestation, and the fate of the Amazon. *Science* 319, 169–172. <https://doi.org/10.1126/science.1146961>
- Malhi, Y., Wood, D., Baker, T.R., Wright, J., Phillips, O.L., Cochrane, T., Meir, P., Chave, J., Almeida, S., Arroyo, L., Higuchi, N., Killeen, T.J., Laurance, S.G., Laurance, W.F., Lewis, S.L., Monteagudo, A., Neill, D.A., Vargas, P.N., Pitman, N.C.A., Quesada, C.A., Salomão, R., Silva, J.N.M., Lezama, A.T., Terborgh, J., Martínez, R.V., Vinceti, B., 2006. The regional variation of aboveground live biomass in old-growth Amazonian forests. *Global Change Biology*. <https://doi.org/10.1111/j.1365-2486.2006.01120.x>
- Marchand, C., 2017. Soil carbon stocks and burial rates along a mangrove forest chronosequence (French Guiana). *Forest Ecology and Management*. <https://doi.org/10.1016/j.foreco.2016.10.030>
- Marchand, C., Lallier-Vergès, E., Baltzer, F., 2003. The composition of sedimentary organic matter in relation to the dynamic features of a mangrove-fringed coast in French Guiana. *Estuarine, Coastal and Shelf Science*. [https://doi.org/10.1016/s0272-7714\(02\)00134-8](https://doi.org/10.1016/s0272-7714(02)00134-8)
- Marchand, C., Lallier-Vergès, E., Baltzer, F., Albéric, P., Cossa, D., Baillif, P., 2006. Heavy metals distribution in mangrove sediments along the mobile coastline

- of French Guiana. Marine Chemistry.
<https://doi.org/10.1016/j.marchem.2005.06.001>
- Marques, J. S.J., Almeida, M. G., Martinelli, L. A., Jones, M. W., Rezende, C.E., (in preparation). Efeito das mudanças da cobertura vegetal na $\delta^{13}\text{C}$ da matéria orgânica no contínuo continente/oceano do rio Paraíba do Sul
- Marques, J.S.J., Dittmar, T., Niggemann, J., Almeida, M.G., Gomez-Saez, G.V., Rezende, C.E., 2017. Dissolved Black Carbon in the Headwaters-to-Ocean Continuum of Paraíba Do Sul River, Brazil. *Frontiers in Earth Science*.
<https://doi.org/10.3389/feart.2017.00011>
- Martinelli, L.A., Nardoto, G.B., Soltangheisi, A., Reis, C.R.G., Abdalla-Filho, A.L., Camargo, P.B., Domingues, T.F., Faria, D., Figueira, A.M., Gomes, T.F., Lins, S.R.M., Mardegan, S.F., Mariano, E., Miatto, R.C., Moraes, R., Moreira, M.Z., Oliveira, R.S., Ometto, J.P.H., Santos, F.L.S., Sena-Souza, J., Silva, D.M.L., Silva, J.C.S., Vieira, S.A., 2021. Determining ecosystem functioning in Brazilian biomes through foliar carbon and nitrogen concentrations and stable isotope ratios. *Biogeochemistry*.
<https://doi.org/10.1007/s10533-020-00714-2>
- Masiello, C.A., 2004. New directions in black carbon organic geochemistry. *Marine Chemistry*. <https://doi.org/10.1016/j.marchem.2004.06.043>
- Matos, C.R.L., Berrêdo, J.F., Machado, W., Sanders, C.J., Metzger, E., Cohen, M.C.L., 2020. Carbon and nutrient accumulation in tropical mangrove creeks, Amazon region. *Marine Geology*.
<https://doi.org/10.1016/j.margeo.2020.106317>
- McKee, B.A., Aller, R.C., Allison, M.A., Bianchi, T.S., Kineke, G.C., 2004. Transport and transformation of dissolved and particulate materials on continental margins influenced by major rivers: benthic boundary layer and seabed processes. *Continental Shelf Research*.
<https://doi.org/10.1016/j.csr.2004.02.009>
- Nakane, M., Ajioka, T., Yamashita, Y., 2017. Distribution and Sources of Dissolved Black Carbon in Surface Waters of the Chukchi Sea, Bering Sea, and the North Pacific Ocean. *Frontiers in Earth Science*.
<https://doi.org/10.3389/feart.2017.00034>

- Nittrouer, C.A., Curtin, T.B., DeMaster, D.J., 1986. Concentration and flux of suspended sediment on the Amazon continental shelf. *Continental Shelf Research*. [https://doi.org/10.1016/0278-4343\(86\)90058-0](https://doi.org/10.1016/0278-4343(86)90058-0)
- Ometto, J.P.H.B., Ometto, J.P.H., Ehleringer, J.R., Domingues, T.F., Berry, J.A., Ishida, F.Y., Mazzi, E., Higuchi, N., Flanagan, L.B., Nardoto, G.B., Martinelli, L.A., n.d. The stable carbon and nitrogen isotopic composition of vegetation in tropical forests of the Amazon Basin, Brazil. *Nitrogen Cycling in the Americas: Natural and Anthropogenic Influences and Controls*. https://doi.org/10.1007/978-1-4020-5517-1_12
- Ovalle, A.R.C., Silva, C.F., Rezende, C.E., Gatts, C.E.N., Suzuki, M.S., Figueiredo, R.O., 2013. Long-term trends in hydrochemistry in the Paraíba do Sul River, southeastern Brazil. *Journal of Hydrology*. <https://doi.org/10.1016/j.jhydrol.2012.12.036>
- Parnell, A.C., Inger, R., Bearhop, S., Jackson, A.L., 2010. Source partitioning using stable isotopes: coping with too much variation. *PLoS One* 5, e9672. <https://doi.org/10.1371/journal.pone.0009672>
- Ray, R., Michaud, E., Aller, R.C., Vantrepotte, V., Gleixner, G., Walcker, R., Devesa, J., Le Goff, M., Morvan, S., Thouzeau, G., 2018. The sources and distribution of carbon (DOC, POC, DIC) in a mangrove dominated estuary (French Guiana, South America). *Biogeochemistry*. <https://doi.org/10.1007/s10533-018-0447-9>
- RC Team. (2018). R Foundation for Statistical Computing, Vienna, Austria, 2018. R: A language and environment for statistical computing.
- Reisser, M., Purves, R.S., Schmidt, M.W.I., Abiven, S., 2016. Pyrogenic Carbon in Soils: A Literature-Based Inventory and a Global Estimation of Its Content in Soil Organic Carbon and Stocks. *Frontiers in Earth Science*. <https://doi.org/10.3389/feart.2016.00080>
- Rezende, C.L., Scarano, F.R., Assad, E.D., Joly, C.A., Metzger, J.P., Strassburg, B.B.N., Tabarelli, M., Fonseca, G.A., Mittermeier, R.A., 2018. From hotspot to hopespot: An opportunity for the Brazilian Atlantic Forest. *Perspectives in Ecology and Conservation*. <https://doi.org/10.1016/j.pecon.2018.10.002>
- Ribas, L. M. (2012). Caracterização de fontes de matéria orgânica do estuário do rio Paraíba do Sul, RJ, Brasil (Doctoral dissertation, Tese de doutorado, Universidade Estadual do Norte Fluminense, 2012. Tese 131p).

- Richard, S., Arnoux, A., Cerdan, P., Reynouard, C., & Horeau, V., 2000. Mercury levels of soils, sediments and fish in French Guiana, South America. *Water, Air, and Soil Pollution*, 124(3), 221-244. <https://doi.org/10.1023/A:1005251016314>
- Richey, J.E., Meade, R.H., Salati, E., Devol, A.H., Nordin, C.F., Dos Santos, U., 1986. Water Discharge and Suspended Sediment Concentrations in the Amazon River: 1982-1984. *Water Resources Research*. <https://doi.org/10.1029/wr022i005p00756>
- Roth, P.J., Lehndorff, E., Brodowski, S., Bornemann, L., Sanchez-García, L., Gustafsson, Ö., Amelung, W., 2012. Differentiation of charcoal, soot and diagenetic carbon in soil: Method comparison and perspectives. *Organic Geochemistry*. <https://doi.org/10.1016/j.orggeochem.2012.01.012>
- Rumpel, C., Ba, A., Darboux, F., Chaplot, V., Planchon, O., 2009. Erosion budget and process selectivity of black carbon at meter scale. *Geoderma*. <https://doi.org/10.1016/j.geoderma.2009.10.006>
- Saiz, G., Wynn, J.G., Wurster, C.M., Goodrick, I., Nelson, P.N., Bird, M.I., 2015. Pyrogenic carbon from tropical savanna burning: production and stable isotope composition. *Biogeosciences*. <https://doi.org/10.5194/bg-12-1849-2015>
- Sánchez-García, L., de Andrés, J.R., Gélinas, Y., Schmidt, M.W.I., Louchouart, P., 2013. Different pools of black carbon in sediments from the Gulf of Cádiz (SW Spain): Method comparison and spatial distribution. *Marine Chemistry*. <https://doi.org/10.1016/j.marchem.2013.02.006>
- Santín, C., Doerr, S.H., Kane, E.S., Masiello, C.A., Ohlson, M., de la Rosa, J.M., Preston, C.M., Dittmar, T., 2016. Towards a global assessment of pyrogenic carbon from vegetation fires. *Glob. Chang. Biol.* 22, 76–91. <https://doi.org/10.1111/gcb.12985>
- Schneider, M.P.W., Smittenberg, R.H., Dittmar, T., Schmidt, M.W.I., 2011. Comparison of gas with liquid chromatography for the determination of benzenepolycarboxylic acids as molecular tracers of black carbon. *Organic Geochemistry*. <https://doi.org/10.1016/j.orggeochem.2011.01.003>
- Shultz, D.J., Calder, J.A., 1976. Organic carbon variations in estuarine sediments. *Geochimica et Cosmochimica Acta*. [https://doi.org/10.1016/0016-7037\(76\)90002-8](https://doi.org/10.1016/0016-7037(76)90002-8)

- Silva, M.A.L., Calasans, C.F., Ovalle, A.R.C., Rezende, C.E., 2001. Dissolved Nitrogen and Phosphorus Dynamics in the Lower Portion of the Paraíba do Sul River, Campos dos Goytacazes, RJ, Brazil. *Brazilian Archives of Biology and Technology*. <https://doi.org/10.1590/s1516-89132001000400006>
- Singh, N., Abiven, S., Torn, M.S., Schmidt, M.W.I., 2012. Fire-derived organic carbon in soil turns over on a centennial scale. *Biogeosciences*. <https://doi.org/10.5194/bg-9-2847-2012>
- Smith, H.G., Sheridan, G.J., Lane, P.N.J., Nyman, P., Haydon, S., 2011. Wildfire effects on water quality in forest catchments: A review with implications for water supply. *Journal of Hydrology*. <https://doi.org/10.1016/j.jhydrol.2010.10.043>
- Solórzano, A., de Assis Brasil, L.S.C., de Oliveira, R.R., 2021. The Atlantic Forest Ecological History: From Pre-colonial Times to the Anthropocene. *The Atlantic Forest*. https://doi.org/10.1007/978-3-030-55322-7_2
- Souza, T.A., Godoy, J.M., Godoy, M.L.D., Moreira, I., Carvalho, Z.L., Salomão, M.S.M., Rezende, C.E., 2010. Use of multitracers for the study of water mixing in the Paraíba do Sul River estuary. *Journal of Environmental Radioactivity*. <https://doi.org/10.1016/j.jenvrad.2009.11.001>
- Stahl, C., Freycon, V., Fontaine, S., Dezécache, C., Ponchant, L., Picon-Cochard, C., Klumpp, K., Soussana, J.-F., Blanfort, V., 2016. Soil carbon stocks after conversion of Amazonian tropical forest to grazed pasture: importance of deep soil layers. *Regional Environmental Change*. <https://doi.org/10.1007/s10113-016-0936-0>
- Stubbins, A., Niggemann, J., Dittmar, T., 2012. Photo-lability of deep ocean dissolved black carbon. *Biogeosciences*. <https://doi.org/10.5194/bg-9-1661-2012>
- Sun, S., Schefuß, E., Mulitza, S., Chiessi, C.M., Sawakuchi, A.O., Zabel, M., Baker, P.A., Hefter, J., Mollenhauer, G., 2017. Origin and processing of terrestrial organic carbon in the Amazon system: lignin phenols in river, shelf, and fan sediments. *Biogeosciences*. <https://doi.org/10.5194/bg-14-2495-2017>
- Trento, A., Vinzón, S., 2014. Experimental modelling of flocculation processes-the case of Paraíba do Sul Estuary. *International Journal of Sediment Research*. [https://doi.org/10.1016/s1001-6279\(14\)60052-4](https://doi.org/10.1016/s1001-6279(14)60052-4)

- Venables, W.N., Ripley, B.D., 2002. Modern Applied Statistics with S. Statistics and Computing. <https://doi.org/10.1007/978-0-387-21706-2>
- Wagner, S., Cawley, K.M., Rosario-Ortiz, F.L., Jaffé, R., 2015. In-stream sources and links between particulate and dissolved black carbon following a wildfire. *Biogeochemistry*. <https://doi.org/10.1007/s10533-015-0088-1>
- Wagner, S., Jaffé, R., Stubbins, A., 2018. Dissolved black carbon in aquatic ecosystems. *Limnology and Oceanography Letters*. <https://doi.org/10.1002/lol2.10076>
- Wanderley, C.V.A., Godoy, J.M., Godoy, M.L.D., Rezende, C.E., Lacerda, L.D., Moreira, I., Carvalho, Z.L., 2013. Evaluating Sedimentation Rates in the Estuary and Shelf Region of the Paraíba do Sul River, Southeastern Brazil. *Journal of the Brazilian Chemical Society*. <https://doi.org/10.5935/0103-5053.20130268>
- Ward, N.D., Krusche, A.V., Sawakuchi, H.O., Brito, D.C., Cunha, A.C., Moura, J.M.S., da Silva, R., Yager, P.L., Keil, R.G., Richey, J.E., 2015. The compositional evolution of dissolved and particulate organic matter along the lower Amazon River—Óbidos to the ocean. *Marine Chemistry*. <https://doi.org/10.1016/j.marchem.2015.06.013>
- Wells, J.T., Coleman, J.M., 1981. Periodic mudflat progradation, northeastern coast of South America; a hypothesis. *Journal of Sedimentary Research*. <https://doi.org/10.2110/jsr.51.1069>
- Werf, G.R. van der, van der Werf, G.R., Randerson, J.T., Giglio, L., van Leeuwen, T.T., Chen, Y., Rogers, B.M., Mu, M., van Marle, M.J.E., Morton, D.C., James Collatz, G., Yokelson, R.J., Kasibhatla, P.S., 2017. Global fire emissions estimates during 1997–2016. *Earth System Science Data*. <https://doi.org/10.5194/essd-9-697-2017>
- Wilkinson, B.H., McElroy, B.J., 2007. The impact of humans on continental erosion and sedimentation. *Geological Society of America Bulletin*. <https://doi.org/10.1130/b25899.1>

SUPPLEMENTARY INFORMATION

Supplementary Table 1. Sampling locations (latitude and longitude), electrical conductivity ($\mu\text{S cm}^{-1}$), carbon and nitrogen isotopic compositions ($\delta^{13}\text{C}$ and $\delta^{15}\text{N}$, respectively), carbon and nitrogen atomic ratio, black carbon content normalized by organic carbon content and degree of condensation (B6CA:B5CA).

Coastal zone	Latitude	Longitude	Electrical conductivity ($\mu\text{S cm}^{-1}$)	$\delta^{13}\text{C}$ (‰)	$\delta^{15}\text{N}$ (‰)	(C:N) _a	BC (mg g^{-1} OC)	Degree of condensation
Sinnamary	5°27'31"N	53°0'24"W	15704	-26.5	3.7	10.61	1.35	0.11
	5°29'9"N	53°0'7"W	19280	-25.3	4.5	7.82	0.08	0.16
	5°28'21"N	53°2'49"W	11314	-26.6	4.2	12.25	0.48	0.41
	5°28'24"N	53°2'16"W	8303	-25.0	3.8	8.76	0.70	0.55
	5°28'23"N	53°2'15"W	12791	-27.7	3.9	11.74	1.72	0.23
	5°27'29"N	53°0'2"W	15704	-25.7	3.6	9.20	0.07	0.18
Amazon	0°10'13"S	47°57'11"W	53300	-25.5	4.0	9.53	0.45	0.29
	0°57'6"N	49°38'52"W	400	-27.6	2.7	9.67	0.55	0.21
	2°5'29"N	47°40'5"W	53800	-20.7	1.8	9.33	0.03	0.16
	0°3'17"N	48°42'22"W	42300	-27.9	3.6	12.62	0.00	0.00
	2°2'3"N	48°49'56"W	8600	-26.5	3.8	9.77	0.17	0.01
	3°33'3"N	50°7'15"W	54000	-24.1	4.6	7.63	0.24	0.44
	1°1'33"N	47°4'1"W	53500	-32.4	3.5	9.10	0.00	0.00
	0°38'39"S	46°46'26"W	44600	-23.1	3.5	9.10	0.00	0.00
1°39'25"N	48°2'14"W	26800	-23.6	1.8	5.83	0.08	0.03	

Continue

2°19'15"N	48°37'54"W	53100	-24.8	2.4	10.30	0.00	0.00	Continued
3°56'56"N	47°36'19"W	53100	-20.7	5.4	7.01	0.72	0.60	
3°5'39"N	50°30'28"W	17600	-24.7	3.1	7.77	0.29	0.58	
1°54'35"N	46°38'25"W	52700	-22.5	4.6	10.04	0.00	0.00	
0°34'3"N	47°59'52"W	32500	-26.2	3.6	9.72	0.00	0.00	
21°38'31"S	41°3'23"W	84	-23.6	6.3	12.34	0.84	0.53	
21°36'27"S	40°59'16"W	36700	-24.6	6.0	12.81	0.34	0.44	
21°36'6"S	41°2'47"W	2790	-22.4	6.6	10.81	0.52	0.60	
21°36'59"S	41°1'57"W	88	-21.6	7.1	11.68	0.18	0.41	
21°35'16"S	41°2'55"W	74	-23.0	6.3	10.45	0.31	0.40	
21°34'57"S	41°3'10"W	8200	-22.2	6.6	11.47	2.54	0.69	
21°37'2"S	41°1'20"W	108	-21.6	6.8	10.25	0.73	0.63	
21°35'4"S	41°2'40"W	31700	-23.0	5.8	10.03	0.76	0.59	
21°37'3"S	41°0'15"W	638	-24.8	6.6	8.96	2.37	0.16	
21°36'41"S	40°59'42"W	23400	-22.7	5.8	14.73	0.54	0.62	
21°35'16"S	40°57'12"W	45800	-20.6	5.9	11.21	1.11	0.67	
21°31'50S	40°57'55"W	49000	-23.1	6.2	17.37	0.86	0.45	
21°29'1"S	40°49'42"W	51000	-20.4	7.0	10.82	1.28	0.33	

PSR

Supplementary Table 2. Isotopic fractionation factors for carbon and nitrogen isotopic compositions used on the MixSIAR model for each coastal zone.

Isotopic fractionation factors			
Coastal Zone	Source	$\delta^{13}\text{C}$	$\delta^{15}\text{N}$
Sinnamary	Marine	0.915	0.862
	Microphytobenthos	0.800	1.166
	C ₃ Plants	1.167	0.735
Amazon	Marine	0.796	0.985
	C ₃ Plants	1.271	0.637
PSR	Marine	0.842	1.174
	C ₃ Plants	1.385	0.423
	C ₄ Plants	0.589	0.250

4. CONSIDERAÇÕES FINAIS

A importância da obtenção de dados acerca do CN em sedimentos costeiros é de extrema relevância devido a sua representação no ciclo global do carbono e sua presença em todos os compartimentos abióticos, que ainda se tem poucos trabalhos publicados.

5. REFERÊNCIAS BIBLIOGRÁFICAS

- Alexis, M.A., Rasse, D.P., Rumpel, C., Bardoux, G., Péchot, N., Schmalzer, P., Drake, B., Mariotti, A., 2007. Fire impact on C and N losses and charcoal production in a scrub oak ecosystem. *Biogeochemistry*. <https://doi.org/10.1007/s10533-006-9063-1>
- Aufdenkampe, A.K., Mayorga, E., Raymond, P.A., Melack, J.M., Doney, S.C., Alin, S.R., Aalto, R.E., Yoo, K., 2011. Riverine coupling of biogeochemical cycles between land, oceans, and atmosphere. *Frontiers in Ecology and the Environment*. <https://doi.org/10.1890/100014>
- Bird, M.I., Ascough, P.L., 2012. Isotopes in pyrogenic carbon: A review. *Organic Geochemistry*. <https://doi.org/10.1016/j.orggeochem.2010.09.005>
- Brodowski, S., Rodionov, A., Haumaier, L., Glaser, B., Amelung, W., 2005. Revised black carbon assessment using benzene polycarboxylic acids. *Organic Geochemistry*. <https://doi.org/10.1016/j.orggeochem.2005.03.011>
- Brown, R.A., Kercher, A.K., Nguyen, T.H., Nagle, D.C., Ball, W.P., 2006. Production and characterization of synthetic wood chars for use as surrogates for natural sorbents. *Organic Geochemistry*. <https://doi.org/10.1016/j.orggeochem.2005.10.008>
- Budai, A., Calucci, L., Rasse, D.P., Strand, L.T., Pengerud, A., Wiedemeier, D., Abiven, S., Forte, C., 2017. Effects of pyrolysis conditions on Miscanthus and corn cob chars: Characterization by IR, solid state NMR and BPCA analysis. *Journal of Analytical and Applied Pyrolysis*. <https://doi.org/10.1016/j.jaap.2017.09.017>
- Coppola, A.I., Druffel, E.R.M., 2016. Cycling of black carbon in the ocean. *Geophysical Research Letters*. <https://doi.org/10.1002/2016gl068574>

- Coppola, A.I., Wiedemeier, D.B., Galy, V., Haghypour, N., Hanke, U.M., Nascimento, G.S., Usman, M., Blattmann, T.M., Reisser, M., Freymond, C.V., Zhao, M., Voss, B., Wacker, L., Schefuß, E., Peucker-Ehrenbrink, B., Abiven, S., Schmidt, M.W.I., Eglinton, T.I., 2018. Publisher Correction: Global-scale evidence for the refractory nature of riverine black carbon. *Nature Geoscience*. <https://doi.org/10.1038/s41561-018-0252-z>
- Coppola, A.I., Ziolkowski, L.A., Masiello, C.A., Druffel, E.R.M., 2014. Aged black carbon in marine sediments and sinking particles. *Geophysical Research Letters*. <https://doi.org/10.1002/2013gl059068>
- Dittmar, T., 2008. The molecular level determination of black carbon in marine dissolved organic matter. *Organic Geochemistry*. <https://doi.org/10.1016/j.orggeochem.2008.01.015>
- Dittmar, T., de Rezende, C.E., Manecki, M., Niggemann, J., Ovalle, A.R.C., Stubbins, A., Bernardes, M.C., 2012. Continuous flux of dissolved black carbon from a vanished tropical forest biome. *Nature Geoscience*. <https://doi.org/10.1038/ngeo1541>
- Forbes, M.S., Raison, R.J., Skjemstad, J.O., 2006. Formation, transformation and transport of black carbon (charcoal) in terrestrial and aquatic ecosystems. *Sci. Total Environ.* 370, 190–206.
- Glaser, B., Haumaier, L., Guggenberger, G., Zech, W., 1998. Black carbon in soils: the use of benzenecarboxylic acids as specific markers. *Organic Geochemistry*. [https://doi.org/10.1016/s0146-6380\(98\)00194-6](https://doi.org/10.1016/s0146-6380(98)00194-6)
- Goldberg, E.D., 1985. *Black Carbon in the Environment: Properties and Distribution*. Wiley-Interscience.
- Hammes, K., Schmidt, M.W.I., Smernik, R.J., Currie, L.A., Ball, W.P., Nguyen, T.H., Louchouart, P., Houel, S., Gustafsson, Ö., Elmquist, M., Cornelissen, G., Skjemstad, J.O., Masiello, C.A., Song, J., Peng, P., 'an, Mitra, S., Dunn, J.C., Hatcher, P.G., Hockaday, W.C., Smith, D.M., Hartkopf-Fröder, C., Böhmer, A., Luer, B., Huebert, B.J., Amelung, W., Brodowski, S., Huang, L., Zhang, W., Gschwend, P.M., Xanat Flores-Cervantes, D., Largeau, C., Rouzaud, J.-N., Rumpel, C., Guggenberger, G., Kaiser, K., Rodionov, A., Gonzalez-Vila, F.J., Gonzalez-Perez, J.A., de la Rosa, J.M., Manning, D.A.C., López-Capél, E., Ding, L., 2007. Comparison of quantification methods to measure fire-derived (black/elemental) carbon in soils and sediments using reference materials from

- soil, water, sediment and the atmosphere. *Global Biogeochemical Cycles*.
<https://doi.org/10.1029/2006gb002914>
- Hedges, J.I., Eglinton, G., Hatcher, P.G., Kirchman, D.L., Arnosti, C., Derenne, S., Evershed, R.P., Kögel-Knabner, I., de Leeuw, J.W., Littke, R., Michaelis, W., Rullkötter, J., 2000. The molecularly-uncharacterized component of nonliving organic matter in natural environments. *Organic Geochemistry*.
[https://doi.org/10.1016/s0146-6380\(00\)00096-6](https://doi.org/10.1016/s0146-6380(00)00096-6)
- Hockaday, W.C., Grannas, A.M., Kim, S., Hatcher, P.G., 2007. The transformation and mobility of charcoal in a fire-impacted watershed. *Geochimica et Cosmochimica Acta*. <https://doi.org/10.1016/j.gca.2007.02.023>
- Jaffé, R., Ding, Y., Niggemann, J., Vähätalo, A.V., Stubbins, A., Spencer, R.G.M., Campbell, J., Dittmar, T., 2013. Global charcoal mobilization from soils via dissolution and riverine transport to the oceans. *Science* 340, 345–347.
- Jones, M.W., Quine, T.A., de Rezende, C.E., Dittmar, T., Johnson, B., Manecki, M., Marques, J.S.J., de Aragão, L.E.O.C., 2017. Do Regional Aerosols Contribute to the Riverine Export of Dissolved Black Carbon? *Journal of Geophysical Research: Biogeosciences*. <https://doi.org/10.1002/2017jg004126>
- Jones, M.W., Santín, C., van der Werf, G.R., Doerr, S.H., 2020. Publisher Correction: Global fire emissions buffered by the production of pyrogenic carbon. *Nature Geoscience*. <https://doi.org/10.1038/s41561-020-0600-7>
- Kapenberg, A., Blasing, M., Lehndorff, E., Amelung, W., 2016. Black carbon assessment using benzene polycarboxylic acids: Limitations for organic-rich matrices. *Organic Geochemistry*.
<https://doi.org/10.1016/j.orggeochem.2016.01.009>
- Kuhlbusch, T.A.J., Crutzen, P.J., 1995. Toward a global estimate of black carbon in residues of vegetation fires representing a sink of atmospheric CO₂ and a source of O₂. *Global Biogeochemical Cycles*.
<https://doi.org/10.1029/95gb02742>
- Major, J., Lehmann, J., Rondon, M., Goodale, C., 2010. Fate of soil-applied black carbon: downward migration, leaching and soil respiration. *Global Change Biology*. <https://doi.org/10.1111/j.1365-2486.2009.02044.x>
- Masiello, C.A., 2004. New directions in black carbon organic geochemistry. *Marine Chemistry*. <https://doi.org/10.1016/j.marchem.2004.06.043>

- Middelburg, J.J., Nieuwenhuize, J., van Breugel, P., 1999. Black carbon in marine sediments. *Marine Chemistry*. [https://doi.org/10.1016/s0304-4203\(99\)00005-5](https://doi.org/10.1016/s0304-4203(99)00005-5)
- Randerson, J.T., Chen, Y., van der Werf, G.R., Rogers, B.M., Morton, D.C., 2012. Global burned area and biomass burning emissions from small fires. *Journal of Geophysical Research: Biogeosciences*. <https://doi.org/10.1029/2012jg002128>
- Regnier, P., Friedlingstein, P., Ciais, P., Mackenzie, F.T., Gruber, N., Janssens, I.A., Laruelle, G.G., Lauerwald, R., Luysaert, S., Andersson, A.J., Arndt, S., Arnosti, C., Borges, A.V., Dale, A.W., Gallego-Sala, A., Godd ris, Y., Goossens, N., Hartmann, J., Heinze, C., Ilyina, T., Joos, F., LaRowe, D.E., Leifeld, J., Meysman, F.J.R., Munhoven, G., Raymond, P.A., Spahni, R., Suntharalingam, P., Thullner, M., 2013. Anthropogenic perturbation of the carbon fluxes from land to ocean. *Nature Geoscience*. <https://doi.org/10.1038/ngeo1830>
- Reisser, M., Purves, R.S., Schmidt, M.W.I., Abiven, S., 2016. Pyrogenic Carbon in Soils: A Literature-Based Inventory and a Global Estimation of Its Content in Soil Organic Carbon and Stocks. *Frontiers in Earth Science*. <https://doi.org/10.3389/feart.2016.00080>
- S nchez-Garc a, L., de Andr s, J.R., G linas, Y., Schmidt, M.W.I., Louchouart, P., 2013. Different pools of black carbon in sediments from the Gulf of C diz (SW Spain): Method comparison and spatial distribution. *Marine Chemistry*. <https://doi.org/10.1016/j.marchem.2013.02.006>
- Sant n, C., Doerr, S.H., Kane, E.S., Masiello, C.A., Ohlson, M., de la Rosa, J.M., Preston, C.M., Dittmar, T., 2016. Towards a global assessment of pyrogenic carbon from vegetation fires. *Glob. Chang. Biol.* 22, 76–91.
- Schmidt, M.W.I., Noack, A.G., 2000. Black carbon in soils and sediments: Analysis, distribution, implications, and current challenges. *Global Biogeochemical Cycles*. <https://doi.org/10.1029/1999gb001208>
- Schneider, M.P.W., Hilf, M., Vogt, U.F., Schmidt, M.W.I., 2010. The benzene polycarboxylic acid (BPCA) pattern of wood pyrolyzed between 200 C and 1000 C. *Organic Geochemistry*. <https://doi.org/10.1016/j.orggeochem.2010.07.001>
- Singh, N., Abiven, S., Torn, M.S., Schmidt, M.W.I., 2012. Fire-derived organic carbon in soil turns over on a centennial scale. *Biogeosciences*. <https://doi.org/10.5194/bg-9-2847-2012>

- Stock, B. C., & Semmens, B. X. (2016). MixSIAR GUI user manual v3. 1. *Scripps Institution of Oceanography, UC San Diego, San Diego, California, USA.*
- Wang, D., Zhang, W., Hao, X., Zhou, D., 2013. Transport of Biochar Particles in Saturated Granular Media: Effects of Pyrolysis Temperature and Particle Size. *Environmental Science & Technology.* <https://doi.org/10.1021/es303794d>
- Wang, J., Xiong, Z., Kuzyakov, Y., 2016. Biochar stability in soil: meta-analysis of decomposition and priming effects. *GCB Bioenergy.* <https://doi.org/10.1111/gcbb.12266>
- Wolf, M., Lehndorff, E., Wiesenberg, G.L.B., Stockhausen, M., Schwark, L., Amelung, W., 2013. Towards reconstruction of past fire regimes from geochemical analysis of charcoal. *Organic Geochemistry.* <https://doi.org/10.1016/j.orggeochem.2012.11.002>